January 2016

RELATIONSHIPS BETWEEN DIETARY FIBER STRUCTURAL FEATURES AND GROWTH AND UTILIZATION PATTERNS OF HUMAN GUT BACTERIA

Xin Nie
Purdue University

Graduate School Form
30 Updated 12/26/2015

PURDUE UNIVERSITY
GRADUATE SCHOOL
Thesis/Dissertation Acceptance

This is to certify that the thesis/dissertation prepared

By Xin Nie

Entitled
RELATIONSHIPS BETWEEN DIETARY FIBER STRUCTURAL FEATURES AND GROWTH AND UTILIZATION PATTERNS OF HUMAN GUT BACTERIA

For the degree of Doctor of Philosophy

Is approved by the final examining committee:

Bruce R. Hamaker
Chair

Bradley L. Reuhs

John A. Patterson

Eric C. Martens

To the best of my knowledge and as understood by the student in the Thesis/Dissertation Agreement, Publication Delay, and Certification Disclaimer (Graduate School Form 32), this thesis/dissertation adheres to the provisions of Purdue University's "Policy of Integrity in Research" and the use of copyright material.

Approved by Major Professor(s): Bruce R. Hamaker

Approved by: Carlos M. Corvalan 12/02/2016

Head of the Departmental Graduate Program Date

RELATIONSHIPS BETWEEN DIETARY FIBER STRUCTURAL FEATURES AND GROWTH AND UTILIZATION PATTERNS OF HUMAN GUT BACTERIA

A Dissertation

Submitted to the Faculty

of

Purdue University

by

Xin Nie

In Partial Fulfillment of the

Requirements for the Degree

of

Doctor of Philosophy

December 2016

Purdue University

West Lafayette, Indiana

Dedicated to my family and my love

ACKNOWLEDGEMENTS

Thanks to my major professor Dr. Bruce R. Hamaker. This work cannot be finished without your support and help.

Thanks to my committee members Dr. Bradley L. Reuhs, Dr. John A. Patterson and Dr. Eric C. Martens. You are all so nice and always ready to help me.

Special thanks to Dr. Martens. The experience in your lab is great and I would like to thank the members in your lab as well.

Thanks to my lab-mates. You are a great part of my life at Purdue. Thank you for all of the discussion and support.

Thanks to my family.

TABLE OF CONTENTS

Page

Page

Page

Page

LIST OF TABLES

LIST OF FIGURES

Figure Page

ABSTRACT

Nie, Xin. Ph.D., Purdue University, December 2016. Relationship between Dietary Fiber Structural Features and Growth and Utilization Patterns of Human Gut Bacteria. Major Professor: Bruce R. Hamaker. Co-advisor: Bradley L. Reuhs.

Intake of dietary fiber is considered an essential strategy to influence gut microbiota, which is associated with many diet-related chronic diseases such as obesity, diabetes, and inflammatory bowel diseases. In order to make a better choice of dietary fiber for a desired microbiota shift related to a health outcome, knowledge of fiber degradation and utilization by gut bacteria is critical. However, it is still unclear how specific dietary fiber structures may influence the growth of target bacteria.

In this thesis, arabinoxylan (CAX) from corn bran was applied as a model fiber and a range of hydrolyzate structures were made differing in structural complexity to use as tools to investigate gut bacteria utilization and competition. The first study investigated the structural parameters in fiber molecules, which may be related to bacterial utilization, such as different molecular size, and branch features including type (i.e. mono- and disaccharide branches), density of substitution, and linkage patterns. In the second study, modified discrete hydrolyzate structures with subtly changed arabinosyl branches markedly delayed the lag phase of *Bacteroides xylanisolvens* XB1A (*B. xylanisolvens*) (up to 6 h), a key

member of the gut microbiota, though not of two other xylan degraders, *Bacteroides ovatus* 3-1-23 (*B. ovatus*) and *Bacteroides cellulosyliticus*.DSM 14838 (*B. cell*). This, in turn, decreased the competitiveness of *B. xylanisolvens* in an artificial community additionally containing the other bacteria resulting in notable alterations of the community composition. Small changes in arabinoxylan branched structure, as well as increase in degree of branching and linkage combinations, suppressed the growth of *B. xylanisolvens* in the competitive community environment. Thus, changes in structural complexity of the fiber either conceivably could be used to promote or suppress target bacteria. Further work showed that transcription of arabinoxylan utilization genes in *B. xylanisolvens* was similarly delayed for the CAX hydrolysates. Subsequently, the influence of fiber structures on interactions of the same gut bacteria was studied in the artificial microbial community. *B. ovatus* survived on complex fiber structures that itself could not utilize when in the presence of *B. xylanisolvens*. Though such cross-feeding has been demonstrated before, this work showed further that bacteria cross-feed when they are required to do so, and when another utilizable substrate is there they do so to a much lesser extent. Accordingly, while on relatively simple substrates that *B. ovatus* can utilize, the cooperation between two bacteria was markedly reduced, suggesting a fiber structure-dependent survival strategy. The results suggest that it may be possible to achieve rationale interventions in microbiota species composition by identifying discrete fiber structures that are only used by particular bacterial species.

INTRODUCTION

Gut microbiota alterations and human health

Accumulated studies have shown the association between the dysbiosis of gut microbiota and many chronic diseases, such as obesity, type 2 diabetes, inflammatory bowel disease and colon cancer (Joossens et al., 2011; Vijay-Kumar et al., 2010). For instance, in the case of obesity, it is reported that microbial genes gave higher accuracy (90%) than looking at human genes (58%) when categorizing the lean people from the obese ones, indicating gut microbiota could be a better marker in diseases like obesity (Walters et al., 2014). Moreover, a study using germ-free mice demonstrated that disordered microbiota from obese people is responsible for their higher body weight compared to mice with microbiota from healthy people, suggesting the effect of gut microbiota on metabolic functions in humans (Turnbaugh et al., 2006).

In recent years, gut microbiota has been recognized to influence the immune function of the human body (Belkaid & Hand, 2014). Short chain fatty acids (SCFAs) produced by gut microbes from dietary fiber have been proven to play a significant role in the communication between gut microbiota and the host immune system. For instance, acetate and propionate serve as ligands of GPR43, a critical G protein-coupled receptor, which is tightly associated with altered inflammatory response in human gut

(Brown et al., 2003). Butyrate is also the primary energy source for colonocytes related to epithelium maintenance (Ahmad et al., 2000). In addition, it has been shown that bacteria from *Bacteroidetes* can use carbon source such as glucose for the synthesis of glycans. For example, *Bacteroides fragilis*, a commensal bacteria, produces a glycan called polysaccharide A that has demonstrated anti-inflammatory effects in mice (Troy & Kasper, 2010).

Therefore, a good balance of gut microbiota is of importance for immune function in human body, suggesting manipulation of the microbiota as a novel strategy for prevention or reduction of the risk of the chronic diseases discussed above. Several promising approaches have been reported such as probiotics, fecal transplantation, and consumption of prebiotics represented by dietary fiber.

Dietary fiber intervention for microbiota symbiosis

Dietary fiber intervention is considered a promising and practical strategy to improve the colonic microbiota of consumers. On one hand, researchers have demonstrated that decreased dietary fiber consumption is responsible for the disorders of the human gut microbiome and even depletions of some gut bacteria in modern society (Conlon, 2015; Sonnenburg et al., 2016). Additionally, high fiber diets showed positive effect on improvement of gut microbiota on diversity or specific bacteria promotions for human health, known as prebiotics (Bindels et al., 2015; Verspreet et al., 2016). On the other hand, both probiotics and fecal transplantation samples require appropriate fiber for their metabolism and survival in the gut environment. Therefore, how to choose proper dietary

fiber substrates for personalized requirements of consumers would always be a core issue in the area.

Alkaline extracted corn bran arabinoxylan as a model fiber

Corn arabinoxylan, as one of the hemicelluloses, provides high propionate-stimulating effect, indicating it can be a potential prebiotic candidate. In addition, corn arabinoxylan shows an obvious initial slow fermentation property, which may be related to its high degree and complexity of branched structures. The basic chemical model of arabinoxylan is composed of a linear *β*-1, 4-linked Xyl*p* backbone, with the side chain substituted Ara*f* residues at some O-2 and /or O-3 positions. Additionally, for corn arabinoxylans, terminal xylose units exist on mono- and disaccharide branch chains, and they also can contain galactose and glucuronic acid. In previous work in our lab, repeating structures varying in side chain density and complexity were found on the corn xylan backbone, showing that different regions favor different bacteria. Those structural properties of corn arabinoxylan make it a good model molecule to produce a range of hydrolyzates with different structural features, which may align with various polysaccharide utilization systems in different gut bacteria for their specific growth behavior.

Statement of problem

In their genomes, bacteria from *Bacteroidetes* produce carbohydrate-active enzymes (CAZymes), binding proteins, and transporters that together are called polysaccharide utilization loci (PULs) (Martens et al., 2009). PULs encode the machinery to digest and transport different dietary fiber substrates. Knowledge is being accumulated quickly on fiber utilization genetic systems of the human gut bacteria, which have been related to the growth of target bacteria in response to given dietary fiber substrates (Cho & Salyers, 2001; Della et al., 1996; Martens et al., 2009; Xu et al., 2007). However, lack of knowledge on fiber structures and bacterial utilization limits the connection between dietary fiber and the behaviors of desired gut bacteria. A better understanding of the relationship between specific dietary fibers and the growth of gut bacteria is critical to advance the field towards fiber therapy for gut microbiome-related diseases and disorders. In this thesis, the structural parameters in a model dietary fiber were studied to explore specificity of fiber structures to bacteria growth and competition.

In order to reach the stage where dietary fibers can be used to make predicted changes in a gut microbial community, first we must understand how bacteria utilize fiber structures, how they compete for such structures, and how they cooperate with each other. It is probable that bacteria's role in the community is changed when the substrate is changed. There are trillions of microorganisms that reside in human colon, which makes the community complicated to study as a dynamic society (Qin et al., 2010). In this thesis study, an artificial microbial community was built to illustrate the behaviors of bacterial members in the multi-bacteria competitive environment. Specific model fiber structures

were chosen to investigate how detailed structural changes affect utilization and competitiveness with other single bacteria, and ultimately each member's strategy to survive and thrive. In the end, our aim is to make better choices of dietary fibers with specific structural features for desired microbiota community shifts and metabolic outcomes.

Hypotheses and specific objectives

Two specific hypotheses were developed to explore the relationship between dietary fiber structure and growth of gut bacteria.

1. High fiber structural specificity exists such that subtle changes in structural patterns/features could change the growth pattern of a bacteria and its competitiveness. Therefore, the first objective of this thesis was to characterize the structural parameters in corn arabinoxylan hydrolyzates treated with isolated and bacterial intact enzymes (Chapter 2). Based on structural changes, a connection was established between fiber chemical structures and growth changes of gut bacteria in either single cultures or multi-bacterial cultures (Chapter 3).

2. Dietary fiber structures drive strategies of bacteria regarding their need to interact or not with each other for survival and ability to thrive in a competitive environment. In the second objective, three bacteria with different digestion features were combined in the community and, through use of fibers with different defined features and complexity, interactions between bacteria were investigated to

understand the change of their roles on different fiber substrates (Chapter 4). Based on the digestion profiles of bacteria in when given substrates in single, two, and three bacteria systems, it was possible to analyze and find how each member adjusted themselves for growth in the competitive environment (Chapter 3 and 4).

References

Ahmad, M. S., et al. (2000). "Butyrate and glucose metabolism by colonocytes in experimental colitis in mice." Gut **46**(4): 493-499.

Belkaid, Y. and T. W. Hand (2014). "Role of the microbiota in immunity and inflammation." Cell **157**(1): 121-141.

Bindels, L. B., et al. (2015). "Towards a more comprehensive concept for prebiotics." Nature Rev Gastroenterol & Hepatol **12**(5): 303-310.

Brown, A. J., et al. (2003). "The Orphan G protein-coupled receptors GPR41 and GPR43 are activated by propionate and other short chain carboxylic acids." J Biol Chem **278**(13): 11312-11319.

Cho, K. H. and A. A. Salyers (2001). "Biochemical analysis of interactions between outer membrane proteins that contribute to starch utilization by *Bacteroides thetaiotaomicron*." J Bacteriol **183**(24): 7224-7230.

Conlon, M. A. and A. R. Bird (2015). "The impact of diet and lifestyle on gut microbiota and human health." Nutrients **7**(1): 17-44.

Della, J. N. and A. A. Salyers (1996). "Contribution of a neopullulanase, a pullulanase, and an alpha-glucosidase to growth of *Bacteroides thetaiotaomicron* on starch." J Bacteriol **178**(24): 7173-7179.

Joossens, M., et al. (2011). "Dysbiosis of the faecal microbiota in patients with Crohn's disease and their unaffected relatives." Gut **60**(5): 631-637.

Martens, E. C., et al. (2009). "Complex glycan catabolism by the human gut microbiota: the Bacteroidetes sus-like paradigm." J Biol Chem **284**(37): 24673-24677.

Qin, J. J., et al. (2010). "A human gut microbial gene catalogue established by metagenomic sequencing." Nature **464**(7285): 59-U70.

Sonnenburg, E. D., et al. (2016). "Diet-induced extinctions in the gut microbiota compound over generations." Nature **529**(7585): 212-U208.

Troy, E. B. and D. L. Kasper (2010). "Beneficial effects of *Bacteroides fragilis* polysaccharides on the immune system." Front Biosci (Landmark Ed) **15**: 25-34.

Turnbaugh, P. J., et al. (2006). "An obesity-associated gut microbiome with increased capacity for energy harvest." Nature **444**(7122): 1027-1031.

Verspreet, J., et al. (2016). "A critical look at prebiotics within the dietary fiber concept." Ann Rev Fd Sci Technol, Vol 7 **7**: 167-190.

Vijay-Kumar, M., et al. (2010). "Metabolic syndrome and altered gut microbiota in mice acking Toll-Like Receptor 5." Science **328**(5975): 228-231.

Walters, W. A., et al. (2014). "Meta-analyses of human gut microbes associated with obesity and IBD." Febs Lett **588**(22): 4223-4233.

Xu, J., et al. (2007). "Evolution of symbiotic bacteria in the distal human intestine." PLoS Biol **5**(7): 1574-1586.

CHAPTER 1. LITERATURE REVIEW: IMPACT OF DIETARY FIBER ON DESIRED GUT MICROBIOTA STRUCTURES FOR IMPROVED HUMAN HEALTH

1.1 Introduction

There are trillions of microbes, mostly bacteria, which are harbored in human gut, and which are associated with human health. Dysbiotic microbiota has been determined in patients with diet-related chronic diseases and health conditions such as obesity, type 2 diabetes, and inflammatory bowel disease, which are prevalent in modern society and particularly in Western-life style countries (Logan et al., 2016). The composition of the gut bacteria may be different due to various factors including age, genetics, diet, and medications (Lozupone et al., 2012). For instance, dramatically change in the microbiota community is found in the early life where, in infants, it increases the diversity and stability due to environment or association with people. The microbiota of infants is easily changed by breastfeeding status or antibiotic intake, which may induce immunologic problems (Yatsunenko et al., 2012). An understanding of how to modulate change of microbiota is needed to aid in development of therapies related to specific health problems. Attention has been especially directed towards manipulation of gut bacteria through diet (Conlon, 2015). Dietary fiber, which is principally composed of the nondigestible carbohydrates of plants, as a common component in human diet is a main source of nutrients for the gut

microbiota, and when used to promote beneficial bacteria is termed as “prebiotics” (Verspreet et al., 2016).

Microorganisms in the human gut collectively possess effective systems at the gene level to utilize the broad diversity of dietary fibers (Martens et al., 2009). In order to metabolize them, gut bacteria have gene loci encoding related degrading enzymes, binding proteins, and transporters which are termed polysaccharides utilization loci (PULs). The different abilities of gut bacteria to digest dietary fibers, and favoring and disfavoring of different groups of bacteria, can result in variations of microbiota community structures. Bacteria apply different strategies to live and thrive in the competitive gastrointestinal ecosystem including both self-promoting and cooperative relationships (Cuskin et al., 2015; Rakoff-Nahoum et al., 2016). This makes it more difficult to predict how dietary fiber will alter the gut bacteria.

Although there are challenges in figuring out how dietary fibers change the gut microbiota, fiber intervention has a good potential to be used in a targeted sense towards gut health and is a relatively mild approach, compared with drugs, to be used in daily life (Yang et al., 2005). In this review chapter, connections between gut microbiota, dietary fiber, and health will be summarized. In addition, the possibility of a better understanding of the relationship between fiber structure and bacterial change will be explored.

1.2 Association between microbiota and human health

1.2.1 Obesity

Obesity nowadays is a serious public health problem, which increases the risk of type 2 diabetes, cardiovascular disease, and many cancers (Pi-Sunyer, 2009). Related alterations of the gut microbiota have been studied related to the regulation of energy balance, nutrition uptake, and in weight and metabolic disorders. Backhed et al. (2004) showed that germ-free mice with the gut microbiota from obese mice gained 60% extra body fat even under reduced chow consumption during a two-week experiment (Backhed et al., 2004). Further study revealed that the decreased ratio of *Bacteroidetes* and higher *Firmicutes* persisted in the obese group after consuming the same diet and level of activity (Ley et al., 2005). A similar difference of microbiota composition was found in obese and lean humans (Ley et al., 2006).

However, this trend is not always true and in the human study conducted by Schwiertz and Taras, et al., increased *Bacteroidetes* was observed in the obese individuals (Schwiertz et al., 2010). The authors mentioned that it is not the gut bacteria themselves, but the products from their fermentation, short chain fatty acids (SCFAs), that were significant in obesity. They proposed that lean people should have higher ratio of acetate to butyrate and propionate than obese people. Further investigation is required on the role of gut microbiota in the development of obesity.

1.2.2 Type 2 diabetes

Type 2 diabetes is a chronic disease that considerably reduces quality of life and increases the risk of heart disease, kidney failure, and overall mortality. It was reported that type 2 diabetes may be related to a decrease of *Bacteroidetes*/*Firmicutes* ratio (Kootte et al., 2012), which is similar to obesity. At the same time, some functional bacteria such as *Bifidobacteria* were decreased and more endotoxin-producing bacteria were found in patients (Festi et al., 2014). It has been shown that microbiota contributing to good intestinal barrier function, such as butyrate-generating species were found beneficial for the treatment of type 2 diabetes (Orel & Trop, 2014).

1.2.3 Inflammatory bowel disease (IBD)

The precise role of the microbiota in the etiology of these diseases is still unclear. However, the microbiota has been shown to promote the inflammatory effects by activating pathogenic T cells and causing intestinal inflammation (Abraham & Medzhitov, 2011). Willing et al. showed that there is decreased microbial diversity and increased *Enterobacteriaceae* including *Escherichia coli*, and *Ruminococcus gnavus* (high mucolytic activities) in patients with IBD, indicating the link between microbiota composition and development of IBD (Willing et al., 2010). Furthermore, in patients with active IBD, there is reduced abundance of the phyla *Firmicutes*, especially *Faecalibacterium prausnitzii*, as well as increased number of bacteria from *Bacteroidetes*. Our knowledge on how microbiota alterations associate with health problems is still restricted. Cooperation

between disciplines will be required to gain different perspectives on how to solve such problems.

1.3 Approaches for manipulation of gut microbiota

1.3.1 Prebiotics

The concept of prebiotics was first introduced by Gibson and Roberfroid in 1995, as 'a nondigestible food ingredient that beneficially affects the host by selectively stimulating the growth and/or activity of one or a limited number of bacteria in the colon, and thus improves host health' (Gibson & Roberfroid, 1995). This term prebiotic was further defined from the microbiota aspect, proposing that the distinction between good and bad bacteria is not yet clear, as are nondigestible compounds that change the structure or activity of the gut microbiota for a beneficial physiological effect (Bindels et al., 2015). More and more dietary carbohydrates have been found with prebiotic potential, such as fructo-, galacto- and arabinoxylano-oligosaccharides (Conway, 2001; Cummings et al., 2001; de Vrese & Schrezenmeir, 2008; Figueroa-Gonzalez, 2011; Fuentes-Zaragoza, 2011; Rastall & Maitin, 2002; Roberfroid et al., 2010).

1.3.2 Probiotics

Probiotics are beneficial microorganisms that are used to influence the gut microbiota structure, metabolic activity, and immune response for host health (Hemarajata

& Versalovic, 2013). The functions of probiotics come from the direct activity of the bacteria or from their products, but perhaps also from the effect on resident microbiota. Probiotics may change the diversity of resident microbes, or stimulate the production of SCFAs for other benefits such as anti-inflammatory effects (Gerritsen et al., 2011). Probiotics should be originally from the human and have the ability to survive in new large intestinal environments (Hemarajata & Versalovic, 2013).

1.3.3 Fecal transplantation

Fecal transplantation is also known as fecal microbial therapy, which uses stool from healthy donors and transplant into target individual for treatment. A dramatic increase in reports of fecal transplantation has taken place since 2000, particularly to treat severe diarrhea induced by overuse or misuse of antibiotics, either accompanied by or a separate bloom of *Clostridium difficile* (*C. difficile*). For instance, Van Nood et al. applied fecal samples to treat the patients with recurrent *C. difficile* and an altered microbiota was observed with increased microbial diversity, increased species such as *Bacteroidetes* and *Clostridium*, and decreased *Proteobacteria* , although this study showed a relatively low cure rate (van Nood, 2013). Good results were obtained on *C. difficile* treatment by other groups (Bakken et al., 2011; Surawicz et al., 2013). In addition, given that fecal transplantation can be effectively on many diseases and its adverse effect is not a problem, the authors recommended to treat fecal as a human tissue not a drug (Smith et al., 2014).

1.4 Dietary fiber and microbiota

Dietary fibers are the nondigestible carbohydrate polymers which can pass through the human upper gastrointestinal tract resulting in change of nutrient absorption and/or gut metabolism. Verspreet et al. showed that dietary fiber can be divided into two categories according to its physiochemical properties such as water-insoluble fiber (i.e. cellulose and water-unextractable arabinoxylan) and water-soluble fiber which can be further classified as viscous fiber like pectin and nonviscous fiber such as arabinoxylan oligosaccharides (Verspreet et al., 2016). Dietary fiber has been shown to benefit consumers by altering the composition of gut microbiota. For instance, inulin stimulates the growth of *Bifidobacteria* and depresses the growth of pathogens *Listeria,* and *E. coli* for improvement of colon health (Orel & Trop, 2014).

The effect of dietary fiber on the alteration of gut bacteria may be influenced by many factors such as the immense diversity of gut microbiota, individual variation, and temporal changes especially during illness. For example, the intestinal microbiota of children from Europe and rural Africa, who were exposed to a modern Western diet and a rural diet respectively, exhibited significant differences in microbial composition (De Filippo, 2010). The major difference is that rural African children have microbiota enriched in *Bacteroidetes* and depleted in *Firmicutes* in comparison to European children. Therefore, deeper understanding on fiber/bacteria relationships may contribute to personalized fiber intake recommendation depending on specific requirements.

1.4.1 Fiber structures for utilization by gut bacteria

As the major carbon source of the growth of gut microbiota, dietary fiber is considered a significant driving force for the change of microbiota in diet (Neyrinck et al., 2012; Walker et al., 2011; Zhao, 2013). For degradation of broadly diverse dietary fiber structures, the gene systems in gut bacteria have been developed. In the phylum *Bacteroidetes*, Salyers et al. reported how *B. thetaiotaomicron* digests starch through a glycan acquisition system, termed the starch utilization system (Sus), which is found to be universal among *Bacteroidetes* (Cho & Salyers, 2001). More and more Sus-like systems have been reported in gut bacteria for utilization of other polysaccharides (Martens et al., 2009). With the systems, gut bacteria encode carbohydrate-active enzymes (CAZymes) for cleavage of linkage types and associated proteins such as carbohydrate-binding proteins and transporters, according to the structural features of the fiber substrates (Lombard et al., 2014). The connections between the PULs in bacteria and dietary fiber structures are still being investigated. Recent study pointed out that not just the composition of the structural units, but the complexity of the branches of xylans affect the regulation of different PULs systems in the same bacteria (Rogowski et al., 2015). Therefore, a better understanding of the function of dietary fiber structures is required to figure out the real connections between fiber features and the behaviors of bacterial growth. And due to the diversity of structures, dietary fiber could be an effective tool for the manipulation of the growth of gut microbes.

Martens et al. (2011) showed that a fructose-sensing hybrid two-component system (HTCs) binds a simpler monosaccharide signal for recognition (Martens et al., 2011). Interestingly, when the structures of fiber start to becoming complex (from

oligosaccharides to polysaccharides), all of the HTCs sensors interact with oligosaccharides for the specific recognition involving both sugar content and linkages. The next question might be whether more structural parameters get involved when the bacterial strains utilize more complex structures and what will be the parameters.

In addition, Vuyst et al. (Riviere et al., 2014) showed that bifidobacterial strains degrade arabinoxylan oligosaccharides (AXOS) through a strain-dependent process which means bifidobacterial strains from different clusters digest different parts of AXOS. This mechanism of AXOS degradation could avoid competition between clusters and favor coexistence. Therefore, modification of patterns will be a reasonable way to favor specific bacterial clusters. Thirty-six strains from 11 species were divided into five clusters based on their target structures in arabinoxylan fragment molecules. The results indicate that preference has nothing to do with species, but instead strains.

It was reported that strains in cluster I (Riviere et al., 2014) could not utilize the xylose backbone or substituents of AXOS, representing by *B. bifidum* LMG 11583; cluster II strains prefer arabinose substituents including *B. longum* subsp. *longum* NCC2705 and other seven strains; strains from cluster III are xylose backbone degraders, but are limited by substituents; cluster IV will digest arabinose substituents first then other parts and cluster V has ability to digest arabinose substituents like II and IV. Another study of human fecal fermentation showed cross-feeding between three bifidobacterial strains which improved the growth of species (Picard, 2005).

1.4.2 *Bacteroidetes* as gut bacteria model

The phylum of *Bacteroidetes* is one of the major members of the microbiota in the human gastrointestinal tract. Carbohydrate-active enzymes were found through the sequencing of *Bacteroidetes* member genomes for the digestion of a large spectrum of dietary fiber substrates. In addition, the specific PULs are shared between the members in the phylum as described above. Altered *Bacteroidetes* have been reported that play a significant role in diseases such as obesity (Ley et al., 2006) and diabetes (Kootte et al., 2012).

1.4.3 Corn arabinoxylan as a dietary fiber model

Corn arabinoxylan, which is extracted from corn bran inalkaline conditions, contains a variety of complex branches and has relatively homogeneous molecular features. There are three types of arabinose residues found in molecules: terminal (60%), 2-linked (22%), and 3-linked (15%). Xylose residues are around 15% unsubstituted type, 40% of mono-substituted type, 20% of di-substituted type, and 20% terminal ones, which makes a unique structural feature of corn arabinoxylan compared to those from other cereals such as wheat, rice and sorghum (Chanliaud, 1995). Enzymatic hydrolysis of corn arabinoxylan with bacterial endoxylanase generates a series of oligosaccharides and larger degraded polymers which contain part of the xylan backbone linked with several different branch types. The complexity of corn arabinoxylan and the effects of fermentation have been studied in previous work in our laboratory (Rumpagaporn et al., 2015; Xu, 2012).

1.5 Conclusions

The relationship between dietary fibers and change of gut microbiota is a fundament of diet intervention against the related chronic non-communicable diseases. More and more studies have been conducted on the utilization systems of gut bacteria and shifts of gut microbiota by high fiber diets, which have encouraged further studies on dietary fiber types and targeted function (Chung et al., 2016; Krajmalnik-Brown, 2012). The knowledge on how specific fiber structures influence change of bacteria is still limited. Here, the question is posed whether it is possible to manipulate the growth of gut bacteria using selected dietary fiber substrates. In order to do so, a better view of dietary fiber structures and how bacteria utilize and compete on them is necessary.

In addition, it is of significance to further investigate the basic rules on the alteration of microbiota composition by interventions like fiber. It is still difficult to illustrate each factor responsible for the poor predictive outcomes of fiber in the gut, however, greater understanding of changes of microbiota due to fibers at a fundamental level would contribute to an understanding of how to use dietary fibers in a more precise way for health. Elucidation of the connections between dietary fiber and gut bacterial growth will improve the efficiency of other therapeutic approaches such as probiotics and fecal transplantation as well.

1.6 References

Abraham, C. and R. Medzhitov (2011). "interactions between the host innate immune system and microbes in inflammatory bowel disease." Gastroenterology **140**(6): 1729-1737.

Backhed, F., et al. (2004). "The gut microbiota as an environmental factor that regulates fat storage." Proc Natl Acad Sci USA **101**(44): 15718-15723.

Bakken, J. S., et al. (2011). "Treating *Clostridium* difficile infection with fecal microbiota transplantation." Clin Gastroenterol Hepatol **9**(12): 1044-1049.

Bindels, L. B., et al. (2015). "Towards a more comprehensive concept for prebiotics." Nature Rev Gastroenterol & Hepatol **12**(5): 303-310.

Chanliaud, E., et al. (1995). "Alkaline extraction and characterization of heteroxylans from maize bran." J Cereal Sci **21**(2): 195-203.

Cho, K. H. and A. A. Salyers (2001). "Biochemical analysis of interactions between outer membrane proteins that contribute to starch utilization by *Bacteroides thetaiotaomicron*." J Bacteriol **183**(24): 7224-7230.

Chung, W. S. F., et al. (2016). "Modulation of the human gut microbiota by dietary fibres occurs at the species level." BMC Biol **14**.

Conlon, M. A. and A. R. Bird (2015). "The impact of diet and lifestyle on gut microbiota and human health." Nutrients **7**(1): 17-44.

Connor, S. J., et al. (2001). "Amelioration of TNBS colitis in mice using prebiotics." Gastroenterology **120**(5): A82-A82.

Conway, P. L. (2001). "Prebiotics and human health: The state-of-the-art and future perspectives." J Nutr **45**: 13-21.

Cummings, J. H., et al. (2001). "A study of fructo-oligosaccharides in the prevention of travellers' diarrhoea." Alimen Pharmacol Ther **15**(8): 1139-1145.

Cuskin, F., et al. (2015). "Human gut Bacteroidetes can utilize yeast mannan through a selfish mechanism." Nature **520**(7547).

De Filippo, C., et al. (2010). "Impact of diet in shaping gut microbiota revealed by a comparative study in children from Europe and rural Africa." Proc Natl Acad Sci USA **107**(33): 14691-14696.

de Vrese, M. and J. Schrezenmeir (2008). "Probiotics, prebiotics, and synbiotics." Food Biotechnol **111**: 1-66.

Festi, D., et al. (2014). "Gut microbiota and metabolic syndrome." World J Gastroenterol **20**(43): 16079-16094.

Figueroa-Gonzalez, I., et al. (2011). "Probiotics and prebiotics - perspectives and challenges." J Sci Fd Agric **91**(8): 1341-1348.

Fuentes-Zaragoza, E., et al. (2011). "Resistant starch as prebiotic: A review." Starch-Starke **63**(7): 406-415.

Gareau, M. G., et al. (2010). "Probiotics and the gut microbiota in intestinal health and disease." Nature Rev Gastroenterol Hepatol **7**(9): 503-514.

Gerritsen, J., et al. (2011). "Intestinal microbiota in human health and disease: the impact of probiotics." Genes Nutr **6**(3): 209-240.

Gibson, G. R. and M. B. Roberfroid (1995). "Dietary modulation of the human colonic microbiota - introducing the concept of prebiotics." J Nutr **125**(6): 1401-1412.

Hemarajata, P. and J. Versalovic (2013). "Effects of probiotics on gut microbiota: mechanisms of intestinal immunomodulation and neuromodulation." Thera Adv Gastroenterol **6**(1): 39-51.

Kootte, R. S., et al. (2012). "The therapeutic potential of manipulating gut microbiota in obesity and type 2 diabetes mellitus." Diab Obes Metabol **14**(2): 112-120.

Krajmalnik-Brown, R., et al. (2012). "Effects of gut microbes on nutrient absorption and energy regulation." Nutr Clin Pract **27**(2): 201-214.

Ley, R. E., et al. (2005). "Obesity alters gut microbial ecology." Proc Natl Acad Sci USA **102**(31): 11070-11075.

Ley, R. E., et al. (2006). "Microbial ecology - human gut microbes associated with obesity." Nature **444**(7122): 1022-1023.

Logan, A. C., et al. (2016). "Immune-microbiota interactions: dysbiosis as a global health issue." Curr Aller Asthma Rep **16**(2).

Lombard, V., et al. (2014). "The carbohydrate-active enzymes database (CAZy) in 2013." Nucl Acids Res **42**(D1): D490-D495.

Lozupone, C. A., et al. (2012). "Diversity, stability and resilience of the human gut microbiota." Nature **489**(7415): 220-230.

Martens, E. C., et al. (2009). "Complex glycan catabolism by the human gut microbiota: the Bacteroidetes Sus-like paradigm." J Biol Chem **284**(37): 24673-24677.

Martens, E. C., et al. (2011). "Recognition and degradation of plant cell wall polysaccharides by two human gut symbionts." Plos Biology **9**(12).

Neyrinck, A. M., et al. (2012). "Wheat-derived arabinoxylan oligosaccharides with prebiotic effect increase satietogenic gut peptides and reduce metabolic endotoxemia in diet-induced obese mice." Nutr Diab **2**.

Orel, R. and T. K. Trop (2014). "Intestinal microbiota, probiotics and prebiotics in inflammatory bowel disease." World J Gastroenterol **20**(33): 11505-11524.

Pi-Sunyer, X. (2009). "The medical risks of obesity." Postgrad Med **121**(6): 21-33.

Picard, C., et al. (2005). "Review article: bifidobacteria as probiotic agents - physiological effects and clinical benefits." Alim Pharmacol Thera **22**(6): 495-512.

Rakoff-Nahoum, S., et al. (2016). "The evolution of cooperation within the gut microbiota." Nature **533**(7602): 255.

Rastall, R. A. and V. Maitin (2002). "Prebiotics and synbiotics: towards the next generation." Curr Opin Biotechnol **13**(5): 490-496.

Riviere, A., et al. (2014). "The ability of bifidobacteria to degrade arabinoxylan oligosaccharide constituents and derived oligosaccharides is strain dependent." Appl Environ Microbiol **80**(1): 204-217.

Roberfroid, M., et al. (2010). "Prebiotic effects: metabolic and health benefits." Brit J Nutr **104**: S1-S63.

Rogowski, A., et al. (2015). "Glycan complexity dictates microbial resource allocation in the large intestine. " Nat Commun, **6**, 7481.

Rumpagaporn, P., et al. (2015). "Structural features of soluble cereal arabinoxylan fibers associated with a slow rate of in vitro fermentation by human fecal microbiota." Carbohyd Polym **130**: 191-197.

Schwiertz, A., et al. (2010). "Microbiota and SCFA in lean and overweight healthy subjects." Obesity **18**(1): 190-195.

Smith, M. B., et al. (2014). "Policy: How to regulate faecal transplants." Nature **506**(7488): 290-291.

Surawicz, C. M., et al. (2013). "Guidelines for diagnosis, treatment, and prevention of *Clostridium difficile* infections." Am J Gastroenterol **108**(4): 478-498.

van Nood, E., et al. (2013). "Duodenal infusion of donor feces for recurrent *Clostridium difficile*." New England Journal of Medicine **368**(5): 407-415.

Verspreet, J., et al. (2016). "A critical look at prebiotics within the dietary fiber concept." Annual Rev Food Sci Technol, Vol 7 **7**: 167-190.

Walker, A. W., et al. (2011). "Dominant and diet-responsive groups of bacteria within the human colonic microbiota." ISME J **5**(2): 220-230.

Willing, B. P., et al. (2010). "A pyrosequencing study in twins shows that gastrointestinal microbial profiles vary with inflammatory bowel disease phenotypes." Gastroenterology **139**(6): 1844-U1105.

Xu, H. (2012). "Influence of the structural complexity of cereal arabinoxylans on human fecal fermentation and their degradation mechanism by gut bacteria." Ph.D. thesis, Purdue University.

Yang, G., et al. (2005). "Application of dietary fiber in clinical enteral nutrition: A meta-analysis of randomized controlled trials." World J Gastroenterol **11**(25): 3935-3938.

Yatsunenko, T., et al. (2012). "Human gut microbiome viewed across age and geography." Nature **486**(7402): 222

Zhao, L. P. (2013). "The gut microbiota and obesity: from correlation to causality." Nature Rev Microbiol **11**(9): 639-647.

CHAPTER 2. STRUCTURAL PARAMETERS OF CORN ARABINOXYLAN POLYMERS INTENDED TO EXERT DIFFERENT INFLUENCES ON GUT MICROBES

2.1 Abstract

As the primary energy source of gut bacteria, dietary fiber with broadly diverse structures is considered to be tightly associated with their growth. However, the detailed connection between defined fiber structures and bacterial behavior is still to be determined. Based on the fact that dietary fibers are utilized by gut bacteria using specific sensory and enzyme systems encoded in their respective genome, we asked the question whether there are specific structural features of fibers that are responsible for growth and competitiveness of bacteria. In this chapter, arabinoxylan from corn bran was used as a model fiber structure, from which a variety of polymer hydrolyzates with modified structural properties were derived, such as with different molecular sizes, and polymer branch features including type (i.e. mono- and di-saccharide branches), type of substituents (i.e. unsubstituted, monosubstitued, disubstituted), and linkage patterns. The structural parameters of corn arabinoxylan and its hydrolyzate fraction used in this thesis study are summarized and discussed in this chapter. Experiments focused on the molecular factors within dietary

fibers to better understand, from a fundamental perspective, their potential to promote or suppress bacterial growth, or create shifts in microbiota communities.

2.2 Introduction

Dietary fiber is one of the major factors that shape the structure of gut microbiota, which contribute to human health. In gut bacteria, the activity of genomes encoding dietary fiber related enzymes and transports, termed as polysaccharide utilization loci (PULs), can be influenced when specific fiber substrates are given in the environment (Martens et al., 2009). The transcriptional activities of PULs in *Bacteroides ovatus* ATCC 8483 have been reportedly affected by the complexity of polysaccharides, using arabinoxylan an important dietary fiber in the human diet, as an example (Rogowski et al., 2015). Depending on the accessibility of fiber substrates, two different systems were activated due to different requirements of related enzymes, PUL-XylS is activated in response to the simple linear xylan and PUL-XylL for complex xylan structures (Martens et al., 2011). When the XylS and XylL mutants were grew on various xylans, there were substrate-specific effects, suggesting selectivity exists and may be naturally variable between sources. In addition, the ability of *Bifidobacterium adolescentis* utilizing the products of *B. ovatus* was determined by the complexity of xylan substrates (Riviere et al., 2014). This study implied the opportunity that structural features like structural complexity of dietary fiber, not just fiber type, could influence of the promotion of individual bacteria. Further study is needed to explore the basic connections between fiber structures and bacterial growth.

Dietary fiber has a vast range of structures, which differs primarily due to the type and amount of monosaccharides, linkages, and branch structures. Using arabinoxylan as an example, structural differences between arabinoxylan from corn, wheat, rice and sorghum are significant (Rumpagaporn et al., 2015), showing that branch types and disaccharide branch chains in even highly substituted structures contribute to the slow fermentation properties in *in vitro* fecal microbial fermentation. Molecular size, A/X ratio, and degree of substitution were not shown not related to the fermentation rate. The results emphasize the importance of structural patterns in dietary fiber branches in gut bacterial utilization, and not the whole molecules on the utilization of gut microbiota. Moreover, three-dimentional gel structures in covalently cross-linked arabinoxylan gels with different crosslinking density through oxidative gelation using laccase modulated rate of degradation by bifidobacteria (Martinez-Lopez et al., 2016), indicating a role for spatial structures of fiber molecules in bacterial utilization. As a result, the structural features of dietary fibers influence interactions between fiber polymers and carbohydrate-active enzymes (CAZymes), binding proteins, and transporters of gut bacteria, thus affecting dietary fiber utilization ability of bacteria.

In this study, using corn arabinoxylan as a model fiber structure, a range of polymers with different structural features were prepared and structural features determined using HPSEC, GC, GC-MS, and NMR methods. The structural parameters on the molecular backbones and branches were investigated, which are associated with how bacteria approach and utilize fiber substrates. In addition, viscosity of the produced polymers was also obtained and compared.

2.3 Materials and Methods

2.3.1 Materials

Dry-milled corn bran was from Bunge Milling with particle size < 50 μm (St. Louis, MO). *α*-amylase from *Bacillus licheniformis*, protease from *Bacillus amyloliquefaciens* and other analytical chemicals were purchased from Sigma; Multifect® AXH-d_3, AXH-m, *β*-1, 4-endoxylanase were obtained from Genencor International Inc., Rochester NY as gifts.

Bacteroides ovatus 3-1-23 (*B. ovatus*), one of the members in the phylum *Bacteroidetes*, was from Dr. Eric C. Martens from the Department of Microbiology & Immunology, University of Michigan Medical School, Ann Arbor, MI.

2.3.2 Methods

2.3.2.1 Extraction of corn arabinoxylan

The alkaline-hydrogen peroxide extraction (Doner, 2000) was used as modified by Rose, et al. (Rose et al., 2010) to obtain corn arabinoxylan (CAX). First, corn bran was partially defatted with hexane (bran:hexane, 1:7 [w/v]) for 30 min. Bran was suspended in water (1:9 w/w). Under constant stirring, the mixture was boiled. After that, 4 mL of heat-stable *α*-amylase (150 U, A-3403, Sigma- Aldrich Corp., St. Louis, MO) were added to hydrolyze starch at 90-95 °C for 30 min, and the mixture was cooled in an ice bath to 50 °C.

The pH was adjusted to 6.0, and 5 mL of neutral protease (4 U, P-1236, Sigma-Aldrich) were added to hydrolyze protein at 50 °C for 4 h, and then the mixture was brought to a boil to inactivate the enzymes, cooled in an ice bath, and the pH was adjusted to 7.0. The slurry was centrifuged at 10,000 *g* for 10 min. The residue was washed three times with water, centrifuged, dried in a forced air oven (40 °C, 48 h), and then ground in a cyclone mill. The enzyme-treated bran (50 g) was suspended in 1 L of 1 M sodium hydroxide. Under constant mixing at 60 °C, 42 mL of 30% hydrogen peroxide were slowly added to the mixture, which was stirred for a total of 4 h and then centrifuged (10,000 *g* for 10 min). 3 volumes of ethanol (95% v/v) were added to the supernatant. The mixture was held overnight at 4 °C, and then the aqueous ethanol portion, containing released unbound ferulic acid was siphoned off, discarded, and the precipitated material was washed with 80% ethanol, anhydrous ethanol, and acetone. The resulting powder was air-dried until no solvent could be detected by odor and then further dried in an oven at 40 °C for 24 h. To further purify the alkali-soluble fraction, enzymatic treatments with heat-stable *α*-amylase and neutral protease, ethanol precipitations, and washings were repeated as described above.

2.3.2.2 Enzymatic treatments of corn arabinoxylan

CAX (40 g) was dissolved in 1.5 L of sodium acetate buffer (25 mM, pH ~ 5.0), and 15 ml of Multifect CX XL endoxylanase (445 XAU/ml) was added. The mixture was incubated at 60 °C for 24 h, boiled for 15 min to inactivate the enzymes, and centrifuged at 10,000 *g* for 30 min. Ethanol (4 volumes) was added to the supernatant with stirring to

precipitate the corn hydrolyzate (CH). Then CH was debranched with AXH-d_3 and AXH-m using the method introduced by Sorensen et al. (Sorensen, Meyer, & Pedersen, 2003), with modification (Xu, 2012): 2 g of CH was dissolved in 100 ml of sodium acetate buffer (25 mM, pH 6) and 0.4 ml of AXH-d_3 and AXH-m were added, with constant stirring at 40 °C for 6 h. Different sequences of the debranching and endoxylanase enzymes were applied for different products. After adjusting the pH to 5, the debranched CH was then hydrolyzed by the endoxylanase. CAX was also debranched: 8 g of CAX was dissolved in 400 ml of sodium acetate buffer (25 mM, pH 6) and 1.6 ml of either AXH-d_3 or AXH-m were added, with constant stirring at 40 °C for 6 h. Thereafter, 1.6 ml of the other debranching enzyme was added under the same conditions for an additional 12 h. After adjusting the pH to 5, the debranched CAX was then hydrolyzed by the endoxylanase, as described above. The final fractions obtained were debranched hydrolyzed corn AXs (CAXHs) (Xu, 2012).

2.3.2.3 Bacterial predigestion of complex corn arabinoxylan polymer

$CAXH_2$ (1 g), one of corn AXs from above, was fermented by *B. ovatus* in an anaerobic chamber for 3 d. Supernatant was collected by centrifugation at 1000 *g*. A digestion experiment was performed in *Bacteroides* minimal medium (MM). Final concentrations of common components were: 100 mM KH_2PO_4 (pH 7.2), 15 mM NaCl, 8.5 mM $(NH_4)_2SO_4$, 4 mM L-cysteine, 1.9 μM hematin/200μM L-histidine (prepared together as a 1,000x solution), 100 M $MgCl_2$, 1.4 M $FeSO_4 \cdot 7H_2O$, 50 M $CaCl_2$, 1 g ml^{-1} vitamin K_3, and 5 ng ml^{-1} vitamin B_{12}. Minimal medium was prepared at 10X concentration

and sterilized by filtration (0.22 m pore size). Corn arabinoxylan polymers were added to MM at a final concentration 0.5% (w/v) and were sterilized by autoclaving in distilled water at 1% (w/v). Medium was reduced by adding L-cysteine just before use and immediately placed into the anaerobic chamber (Coy Manufacturing, Grass Lake, MI), and then used within 3 h (Martens et al., 2008).

2.3.2.4 Purification of digested arabinoxylan substrate

The digested sample from above (2.3.2.3) was transferred to 15 ml centrifuge tube and put in a water bath at 65 °C. An equal volume of phenol was dripped into the tuber over a period of 5 min. Samples were then incubated at 65 °C for another 10 min and vortexed once during the period. After cooling down to room temperature, the samples were centrifuged at 4 °C for 15 min at 12,000 *g*. The upper aqueous layer was transferred to another centrifuge tube and the procedure was repeated once. The final upper aqueous layer was transferred to a dialysis bag (2000 Da cut-off) to remove solvent and solutes, including the oligomeric fractions of the digested polysaccharides (with molecular weight below 2000 Da). The purified solution in the dialysis bag was then freeze-dried. The fraction size distribution profile was obtained by high performance size-exclusion chromatography (HPSEC).

2.3.3 Structural characterization of corn arabinoxylan polymers

2.3.3.1 Molecular size by high performance size exclusive chromatography

Molecular size distributions were obtained using a HPSEC system consisting of a pump (Varian 9012, Varian Associates Inc., Walnut Creek, CA), a syringe sample loading injector (model 7125, Rheodyne Inc., Oak Harbor, WA) with a 100 µL sample loop, two columns with Superdex 30 and 200 analytical grade media (separation range Mw= $< 1 \times 10^4$ and 1×10^4 to 6×10^5, respectively) (Amersham Biosciences, Piscataway, NJ), and a refractive index detector (Varian star 9040, Varian Associates Inc., Walnut Creek, CA). Sample solutions (1% w/v) were prepared and injected (300 µl); deionized water with 0.02% sodium azide was used as the eluent (flow rate of 0.4 ml/min). Data were collected with Varian's Star Chromatography Workstation (Version 4.51, Varian Associates Inc., Walnut Creek, CA). The retention times of pullulan standards (Polymer Laboratories, Santa Clara, CA) were used as external standards.

2.3.3.2 Monosaccharide composition analysis

Monosaccharide composition was obtained by the neutral sugar analysis method in AACC International Official Method 32-25 (AACC, 2000), using a smaller sample size (50 mg). Alditol acetates in ethyl acetate were quantified by gas chromatography using a capillary column SP-2330 (SUPELCO, Bellefonte, PA) with the following conditions: injector volume, 2 µl; injector temperature, 240 ºC; detector temperature, 300 ºC; carrier

gas (helium), velocity 1.9 meter/second; split ratio, 1:2; temperature program was 160 ºC for 6 min, then 4 ºC/min to 220 ºC for 4 min, then 3 ºC/min to 240 ºC for 5 min, and then 11 ºC/min to 255 ºC for 5 min.

2.3.3.3 Glycosidic linkage characterization

Linkage analysis was performed by the method of Carpita and Shea (Carpita et al., 1989) with modifications (Xu, 2012): dried samples (3 mg) were dissolved in anhydrous DMSO (300 µl), and methylated. The methylated samples were hydrolyzed using 250 µl of 2 N trifluoroaceticacid (121 ºC for 1 h). The hydrolyzed samples were dissolved in 100 µl of 1M ammonium hydroxide, and 500 µl of DMSO containing 20 mg/ml of sodium borodeuteride was added to reduce the aldyhyde groups. The mixture was incubated at 40 ºC for 90 min and 6-9 drops of glacial acetic acid were added and mixed to stop reduction reaction. 1-Methylimidazole (100 µl) and acetic anhydride (500 µl) were added for acetylation. Partially methylated alditol acetates in acetone were quantified by GC-FID-MS (7890A-5975C MSD, Agilent Technologies, Inc., Santa Clara, CA, USA) using a SP-2330 capillary column (injector volume, 1 µl; injector temperature, 240 ºC; detector temperature, 300 ºC; carrier gas, helium: 1.9 meter/second; split ratio, 100:1; temperature program, 100 ºC for 2 min, 8 ºC/min to 240 ºC for 20 min).

2.3.3.4 NMR spectroscopy

Samples for ^{1}H NMR spectroscopy were prepared by dissolving samples in deuterium oxide (10 mg/mL) for 8 h at room temperature, followed by freeze-drying. The dissolving and freeze-drying steps were repeated twice more, and then spectra were recorded on an 800 MHz spectrometer (Bruker Avance-III-800, Bruker Corporation, Billerica, MA) at room temperature. Partial structural assignments of the peaks were made by comparison with previously published data (Apirattananusorn et al., 2008; Ebringerova et al., 1994; Gruppen et al., 1992; Hoffmann et al., 1992; Hoffmann et al., 1992).

2.3.3.5 Viscosity of corn arabinoxylan

Solutions (5% w/v) of the fiber samples were prepared in purified water and their shear viscosity was measured using a rotational rheometer (AR-G2 Model from TA Instruments, Newcastle, DE). The cone and plate diameters were 40 mm and the gap was set at 0.055 mm. The cone angle was 0.027 radians. Viscosity data were collect in the shear rate range from 1 to 100 s^{-1} at 37 ºC. The sample viscosity used was determined from evaluation of the viscosity at the lowest shear rates and by looking for a constant maximum at the zero-shear rate viscosity.

2.3.3.6 Statistical analyses

Statistical differences were determined using the Statistical Analysis System software package version 9.2 (SAS Institute, Cary, N.C., U.S.A.). Substrate and time were fixed effects of the model and the latter was included as the repeated measurement.

2.4 Results and Discussion

2.4.1 Corn arabinoxylan (CAX) from corn bran by alkaline extraction

In this study, the yield of arabinoxylan from alkaline extraction of corn bran was around 38% (of starting weight, as is basis). Gradient ethanol solutions were used to obtain a relatively homogeneous substrate. The sample used was precipitated within the 40-60% ethanol range, and freeze-dried. From 40 g alkaline-extracted arabinoxylan, 31.8 g arabinoxylan was obtained with a yield of 79.5%.

Eight hydrolyzates were prepared from CAX using isolated enzymatic and bacterial treatments, as shown in Fig. 2.1. Hydrolyzed corn arabinoxylan (CH) was obtained by hydrolyzing CAX using β-1, 4-endoxylanase with a yield of 50.2%. $CAXH_1$ and $CHAXH_1$ were the products of CAX debranched using two arabinofuranosidases, AXH-m and then AXH-d_3, followed by β-1, 4-endoxylanase hydrolysis. AXH-m randomly removes arabinose branches from the mono-substituted backbone unit and AXH-d_3 removes the 3-O position arabinose from the di-substituted xylosyl units on the backbone. $CAXH_2$ and $CHAXH_2$ were obtained using the same enzymes but in the opposite order (AXH-d_3 first,

then AXH-m) and β-1, 4-endoxylanase. $CHAX_1$ and $CHAX_2$ were the structures of $CHAXH_1$ and $CHAXH_2$ before β-1, 4-endoxylanase hydrolysis. $CAXH_2$ was predigested by *Bacteroides ovatus* 3-1-23 to obtain a more complex structure that *B. ovatus* could not then further utilize (CAXH-digest). The yields of the substrates CH, $CAXH_1$, $CAXH_2$, $CHAX_1$ and $CHAX_2$ were below 70%, probably because of the complexity of CAX branches, as mentioned in the previous work from our laboratory (Xu, 2012).

2.4.2 Purification of CAXH-digest

After the predigestion of *Bacteroides ovatus* 3-1-23, three fractions were found using HPSEC, in a ratio of 5: 80:15 (Fig. 2.2). The molecular weight and size distribution of CAX, CAXH, and CAXH-digest are shown in Fig. 2.2. Highest weight-average molecular weight was for CAX (315,500 Da), followed by CAXH (112,700 Da). After *B. ovatus* digestion of CAXH, three major components were collected with average molecular weights of 111,000 Da, 24,200 Da and 3,700 Da. The peak with 111,000 Da was considered to be the native CAXH component of the mixture. For structure analysis, peak 24,200 Da was collected.

2.4.3 Molecular size distribution of CAX hydrolyzates

CAX had an average molecular weight around 315,500 Da, which is similar to the molecular weight Rumpagaporn et al. (2015) reported (360,000 Da) (Rumpagaporn et al., 2015), and larger than what Xu (Xu, 2012) obtained (190,000 Da). The difference occurred

probably due to different efficiency of the *β*-1, 4-endoxylanase which was sourced differently. In addition, the molecular weights of groups $CAXH_1$ and $CAXH_2$, $CHAX_1$ and $CHAX_2$, and $CHAXH_1$ and $CHAXH_2$ are comparable (Table 2.1). The average molecular weight of $CAXH_1$ and $CAXH_2$ (around 112,687 Da) is larger than that of Xu (Xu, 2012) at 19,000 Da.

2.4.4 Neutral sugar composition

As the primary residues in arabinoxylan structures, arabinose and xylose were measured and are summarized in Table 2.2. CAX had the highest A/X ratio of 0.54 and CH is 0.47, showing that their structures keep their branch structures. After debranching, the A/X ratios of hydrolyzates decreased to 0.29 and 0.34, reflecting the loss of arabinose in enzymatic hydrolysis.

2.4.5 Glycosidic linkage profiles of CAX hydrolyzates

As shown in Table 2.3, nine linkages were analyzed for CAX hydrolyzates, mainly focusing on the change of branch residues involving Ara*f* and Xyl*p*. CAX had the smallest amount of unsubstituted Xyl*p* (11.9%) and large amount of terminal residues 15.3% for (Ara*f*)1→ and 22.9% for (Xyl*p*)1→. At the same time, it had around 26.1% of 3-O substituted →4(Xyl*p*)1 →, indicating a highly branched structure. CH had decreased terminal Ara*f* (8.9%), but increased Xyl*p* (23.3%) compared to CAX. In $CAXH_1$ and $CAXH_2$, terminal Ara*f* and Xyl*p* decreased further, but was more unsubstituted →4(Xyl*p*)1

→ because of the effect of debranching enzymes AXH-m and AXH-d_3. But more →2(Ara*f*)1 →, →3(Ara*f*)1 → and →5(Ara*f*)1 → were found in branches to make the molecules relatively complex. $CHAX_1$ and $CHAX_2$ had more unsubstituted →4(Xyl*p*)1 → and less terminal residues compared to other substrates, showing loose molecular structures. $CHAXH_1$ and $CHAXH_2$ had less unsubstituted →4(Xyl*p*)1 → and more terminal Xylp and disubstituted →4(Xyl*p*)1 →, indicating complex molecular features. CAXH-digest showed a large amount of disubstitued →4(Xyl*p*)1 → and disaccharide branch residues →2(Ara*f*)1 →, →3(Ara*f*)1 → and →5(Ara*f*)1 →, representing a highly complex structure.

2.4.6 Features of branches in CAX hydrolyzates

2.4.6.1 Length of substituents (i.e. mono- and disaccharide branches)

This structural parameter refers to the shape of dietary fiber molecules and contributes to difficulty on bacteria to attack fiber backbones. →2(Ara*f*)1 →, →3(Ara*f*)1 → and →5(Ara*f*)1 → in CAX hydrolyzates were only found in branches as part of disaccharide or triaccharide branches, indicating the presence of long branches in the substrates. Terminal residues determined the total amount of branches in molecules. Due to →4 (Xyl*p*) 1 → usually was found on the xylose backbone, we assume the rest of the branches are monosaccharide branches. The results are found in Fig. 2.3.

In general, there was a decrease in monosaccharide branches in higher degree of processing of hydrolyzates, and the proportions of disaccharide branches increased compared to the amount of monosaccharide branches. CAX and CH had more

monosaccharide branches in their molecules, indicating a large and narrow molecular shape compared to other hydrolyzates. For the CAXH-digest, the highest disaccharide branch proportion was obtained suggesting difficulty of bacterial access.

2.4.6.2 Type of substituents (i.e. unsubstituted, monosubstituted, and disubstituted)

How branches are attached on the xylose backbone (i.e. un-, mono-, and di-substituted) relates to the accessibility of substrate for enzymes associated with the gut bacteria. Type of substituents as one of the structural parameters in CAX hydrolyzates is reported in Fig. 2.4. This parameter also represents how loose or dense the branches are on the backbone, which may contribute to how bacteria contact the structure they prefer.

CAX and CH had more unsubstituted and monosubstituted residues than other substrates. $CAXH_1$ and $CAXH_2$, $CHAX_1$ and $CHAX_2$ showed similar proportions of substituents, or degree of substitution. An increase in disubstituted residues on backbones of $CHAXH_1$, $CHAXH_2$ and CAXH-digest was found, indicating increase in density of the branched structures. Because these structures had high amount of disaccharide branches as well, it is reasonable to conclude that they have lower accessibility to bacterial enzymes necessary for degradation and utilization.

2.4.6.3 Linkage patterns

Branch patterns show how branches are arranged on molecular backbones. As we described above, AXH-m was used to randomly remove arabinose residues from the mono-

substituted backbone xylosyl units. AXH-d_3 was used to remove the 3-O position arabinose from di-substituted xylosyl units on the backbone. Different sequential application of AXH-d_3 to remove the 3-O position arabinose from the disubstituted backbone and AXH-m to remove arabinose branches from the mono-substituted backbone unit, was conducted to produce subtly different arrangements of arabinose branches on the xylan backbone. The sequence is significant here because the hydrolysis efficiency of enzymes cannot be 100%, especially on complex structures such as corn arabinoxylan. For instance, 1) if we use AXH-m first, the enzyme needs to access the complex branches to reach the active site so that the hydrolysis of arabinose branches from mono-substituted backbone units will be reduced. Then, when we use AXH-d_3 after this, AXH-d_3 will have more space from the hydrolysis of AXH-m, resulting in a better outcome that breaks the disubstituted branches by removing the 3-O position arabinose and, in turn, produce more 2-O position arabinosyl residues. Oppositely, if we use AXH-d_3 first, the effect that removes arabinose from disubstituted branches will be interrupted and AXH-m will perform better to randomly remove arabinose as single substituents. As a result, more disubstituted branches will be kept compared to the first treatment. Therefore, we expected that $CAXH_1$, the product by the first treatment, has less disubstituents of arabinose and more 2-O position arabinosyl residues. For $CAXH_2$ by treatment 2, there should be more disubstituted branch forms than $CAXH_1$. In the end, compared to $CAXH_1$, $CAXH_2$ is anticipated a higher complexity of branch.

In addition, increase of disubstituted disaccharide branches was found in CAXH-digest compared to $CAXH_2$, the structure before bacterial treatment, which may be significant to obstruct the utilization ability of *B. ovatus* 3-1-23. The decreased

unsubstituted →4 (Xyl*p*) 1 → from $CAXH_2$ to CAXH-digest indicated its importance for *B. ovatus* utilization. Moreover, given the fact that the structure of $CAXH_2$ is hard to be hydrolyzed by isolated enzymes such as (AXH-m, AXH-d_3 and endoxylanase), it is hypothesized that the unsubstituted →4 (Xyl*p*) 1 → units were protected by their neighbors.

2.4.7 Viscosity

Viscosity is about resistance to flow, related to molecular size, and density and flexibility which may influence bacterial digestion. Solutions (5 mg/ml, same concentration as used in the bacterial growth experiments) were analyzed. It was observed that CAX has the highest viscosity of 3.7 cps due to its large molecular size, and CH with 3.4 cps. Three groups, $CAXH_1$ and $_2$, $CHAX_1$ and $_2$, $CHAXH_1$ and $_2$, shared similar viscosities (Table 2.4).

2.4.8 ^{1}H NMR analysis

It is considered that between δ 4.4-5.5 ppm (Gruppen et al., 1992) are the chemical shifts of the anomer hydrogen of arabinoxylan. The region between δ 5.1-5.4 ppm is for *α*-linked Ara*f*, and *β*-linked Xyl*p* is between δ 4.4-4.8 ppm (Apirattananusorn et al., 2008; Ebringerova et al., 1994; Hoffmann et al., 1992). The chemical shift at δ 4.46 ppm represents the linkage of *β*-1, 2, 4-linked Xyl*p*, suggesting the 2-O substituted xylose units (Bendahou et al., 2007; Fischer et al., 2004; Yin et al., 2012). As expected, $CAXH_1$ showed more 2-O substituted xylose units than $CAXH_2$, which is consistent with the discussion

above in session 2.4.6.3 (Fig. 2.5). In the region of α-linked Ara*f,* obviously higher signal was observed in $CAXH_2$ at δ 5.30 ppm than that in $CAXH_1$. According to literature data (Hoffmann, Geijtenbeek, et al., 1992; Hoffmann, Kamerling, et al., 1992), the region around 5.30 and 5.23 ppm is related to the signal of anomeric protons of Ara*f* linked to O-3 and O-2 position on the same Xyl*p* backbone units. The results supported the idea above that $CAXH_2$ has more disubstituted units of arabinose. Additionally, using wheat arabinoxylan, Hoffmann et al. showed that the chemical shift at δ 5.30 ppm indicated the combination of two arabinose disubstituents or one arabinose disubstituent neighboring to another single arabinose substituent (Hoffmann, Geijtenbeek, et al., 1992; Hoffmann, Kamerling, et al., 1992). Accordingly, compared to $CAXH_1$, $CAXH_2$ has a denser and closer branch arrangement. In addition, $CAXH_1$ had stronger signals at δ 4.48 ppm, 4.46 ppm and 3.75 ppm representing more unsubstituted Xyl*p* connected with mono- or unsubstituted Xyl*p*, according to the research by Hoffmann et al., suggesting a relatively open structural feature compared to $CAXH_2$ (Hoffmann, Kamerling, et al., 1992). The results agree with the enzyme functions described above related to linkage patterns.

2.4.9 Models of the difference between $CAXH_1$ and $CAXH_2$

Based on the data above, two possible models on the difference between $CAXH_1$ and $CAXH_2$ were constructed. 1) In the first model as shown in Fig. 2.6a, we assume that there are multiple arabinose residues in the same region of the molecular backbones. There are more 2-O position single arabinose substituents in $CAXH_1$, and may have that single arabinose substituent next to an unsubstituted Xyl*p* unit on backbone. For $CAXH_2$, there

are more disubstituted units, and neighboring to mono- or disubstituents. 2) In the second model in Fig. 2.6b, it is assumed that arabinose branches are in between the long branches (disaccharide branches) and not neighboring to each other. Then the difference between them came from the fact that $CAXH_1$ has more 2-O position single arabinose substituents while $CAXH_2$ has more disubstituents of arabinose residues. Both models support the idea that $CAXH_2$ has relatively denser and more complex linkage patterns than $CAXH_1$. In the molecules of these two substrates, both two models above may exist in different regions in $CAXH_1$ and $CAXH_2$, respectively.

2.5 Conclusions

In this chapter, CAX hydrolyzates were prepared from corn bran using an alkaline extraction method and enzymatic treatments. The complex structures of hydrolyzates decreased the efficiency of enzymes, supporting the idea that structural patterns in dietary fiber molecules, especially branch patterns are important for to their rate and extent of degradation. Structural parameters in CAX hydrolyzates were measured, including molecular size and branch features. According to a previous study, branch patterns play a significant role in gut bacterial fermentation (Rumpagaporn et al., 2015). Therefore, we clarified the branches with mono- and disaccharide branches, and how the branches attach on the xylose backbones of the CAX hydrolyzates. In the hydrolyzates we prepared, $CHAXH_1$, $CHAXH_2$ and CAXH-digest showed high complexity of structure. Linkage profiles supported that they have more disaccharide branches than the other arabinoxylan hydrolyzates. CAX and CH had higher molecular weights resulting in higher viscosity

solutions. NMR results supported that in $CAXH_2$, there are more complex branch patterns involving disubstituents of arabinose residues. While CAXH1 has more 2-O position single arabinose branches for a relatively less complex structure compared to $CAXH_2$.

2.6 References

AACC (2000). "Total dietary fiber - determined as neutral sugar residues, uronic acid residues, and Klason lignin (Uppsala method)." AACC International: Approved Methods of American Association of Cereal Chemists, 10th edition. St. Paul, MN: AACC International Press.

Apirattananusorn, S., et al. (2008). "Chemical, molecular, and structural characterization of alkali extractable nonstarch polysaccharides from Job's tears." J Agric Food Chem **56**(18): 8549-8557.

Bendahou, A., et al. (2007). "Isolation and structural characterization of hemicelluloses from palm of Phoenix dactylifera L." Carbohyd Polym **68**(3): 601-608.

Carpita, N. C., et al. (1989). "Linkage structure of fructans and fructan oligomers from *Triticum*-aestivum and Festuca-arundinacea Leaves." J Plant Physiol **134**(2): 162-168.

Doner, L. W., Sweeney, G. A., & Hicks, K. B. (2000). "Isolation of hemicellulose from corn fiber." USA: Natl Starch and Chem Invest Holding Corp **6**(147): 1-14.

Dubois, M., et al. (1956). "Colorimetric method for determination of sugars and related substances." Anal Chem **28**(3): 350-356.

Ebringerova, A., et al. (1994). "Structural and molecular-properties of a water-soluble arabinoxylan-protein complex isolated from rye bran." Carbohyd Res **264**(1): 97-109.

Fischer, M. H., et al. (2004). "The gel-forming polysaccharide of psyllium husk (Plantago ovata Forsk)." Carbohyd Res **339**(11): 2009-2017.

Gruppen, H., et al. (1992). "Characterization by H-1-Nmr spectroscopy of enzymatically derived oligosaccharides from alkali-extractable wheat-flour arabinoxylan." Carbohyd Res **233**: 45-64.

Hoffmann, R. A., et al. (1992). "H-1-Nmr study of enzymatically generated wheat-endosperm arabinoxylan oligosaccharides - structures of hepta-saccharides to tetradeca-saccharides containing 2 or 3 branched xylose residues." Carbohyd Res **223**: 19-44.

Hoffmann, R. A., et al. (1992). "structural features of a water-soluble arabinoxylan from the endosperm of wheat." Carbohyd Res **226**(2): 303-311.

Martens, E. C., et al. (2008). "Mucosal glycan foraging enhances fitness and transmission of a saccharolytic human gut bacterial symbiont." Cell Host Microbe **4**(5): 447-457.

Martens, E. C., et al. (2009). "Complex glycan catabolism by the human gut microbiota: the Bacteroidetes Sus-like paradigm." J Biol Chem **284**(37): 24673-24677.

Martens, E. C., et al. (2011). "Recognition and degradation of plant cell wall polysaccharides by two human gut symbionts." PLoS Biol, **9**(12), e1001221.

Martinez-Lopez, A. L., et al. (2016). "In vitro degradation of covalently cross-linked arabinoxylan hydrogels by bifidobacteria." Carbohyd Poly **144**: 76-82.

Riviere, A., et al. (2014). "The Ability of Bifidobacteria To Degrade Arabinoxylan Oligosaccharide Constituents and Derived Oligosaccharides Is Strain Dependent." Appl Environ Microbiol **80**(1): 204-217.

Rogowski, A., et al. (2015). "Glycan complexity dictates microbial resource allocation in the large intestine." Nature Comm **6** :7481 doi: 10.1038/ncomms8481.

Rose, D. J., et al. (2010). "Structural differences among alkali-soluble arabinoxylans from maize (*Zea mays*), rice (*Oryza sativa*), and wheat (*Triticum aestivum*) brans influence human fecal fermentation profiles." J Agric Food Chem **58**(1): 493-499.

Rumpagaporn, P., et al. (2015). "Structural features of soluble cereal arabinoxylan fibers associated with a slow rate of in vitro fermentation by human fecal microbiota." Carbohyd Poly **130**: 191-197.

Sorensen, H. R., et al. (2003). "Enzymatic hydrolysis of water-soluble wheat arabinoxylan. 1. Synergy between alpha-L-arabinofuranosidases, endo-1,4-beta-xylanases, and beta-xylosidase activities." Biotechnol Bioeng **81**(6): 726-731.

Xu, H. (2012). "Influence of the structural complexity of cereal arabinoxylans on human fecal fermentation and their degradation mechanism by gut bacteria." Ph.D. thesis, Purdue University.

Yin, J. Y., et al. (2012). "Structural characterization of a highly branched polysaccharide from the seeds of *Plantago asiatica L*." Carbohyd Poly **87**(4): 2416-2424.

2.7 Tables and Figures

Tables

Table 2.1 Composition of corn arabinoxylan enzyme and bacterial produced hydrolyzates.

Sample	Yield %	Average Molecular Weight (Da)
CAX	37.8	315,500
$CAXH_1$	52.1	113,000
$CAXH_2$	55.7	112,700
CAXH-digest	20.2	24,200
CH	50.2	189,600
$CHAX_1$	58.1	153,600
$CHAX_2$	55.3	144,200
$CHAXH_1$	59.1	103,100
$CHAXH_2$	60.2	102,800

Abbreviations: CAX = Corn alkali-extracted arabinoxylans, CH = Corn hydrolyzate obtained by endoxylanase hydrolysis of CAX, $CAXH_1$ = CAX debranched by removing the arabinosyl residues randomly at 2- or 3-monosubstitution, then removed the O-3 position arabinosyl substituent from 2, 3-disubstituion and O-2 arabinosyl substituent was remained as monosubstitution, followed by endoxylanase hydrolysis (termed as DBH_3 in Xu's thesis) (Xu, 2012); $CAXH_2$ = CAX debranched by removing the O-3 position arabinosyl substituent from 2, 3-disubstituion first, then monosubstituents of arabinosyl residues, followed by endoxylanase hydrolysis (termed as DBH_4 in Xu's thesis) (Xu, 2012); CAXH-digest = product of $CAXH_2$ predigested by *B. ovatus* 3-1-23; $CHAX_1$ = CH debranched by removing the arabinosyl residues randomly at 2- or 3-monosubstitution, then removed the O-3 position arabinosyl substituent from 2, 3-disubstituion (termed as HDB_3 in Xu's thesis) (Xu, 2012); $CHAX_2$ = CH debranched by removing the O-3 position arabinosyl substituent from 2, 3-disubstituion first, then monosubstituents of arabinosyl residues (termed as HDB_4 in Xu's thesis) (Xu, 2012); $CHAXH_1$ = product of $CHAX_1$ hydrolyzed by endoxylanase; $CHAXH_2$ =product of $CHAX_2$ hydrolyzed by endoxylanase.

Table 2.2 Sugar composition of CAX hydrolyzates. [a]

Constituent	CAX	CH	$CAXH_1$	$CAXH_2$	$CHAX_1$	$CHAX_2$	$CHAXH_1$	$CHAXH_2$	CAXH-digest
Arabinose	27.4±1.9	22.2±0.8	17.1±1.0	17.5±0.7	14.2±1.2	14.7±0.8	15.0±1.4	14.0±1.2	15.0±1.4
Xylose	51.2±3.0	47.6±4.4	50.2±2.9	52.9±1.8	48.2±2.1	49.1±1.7	44.3±1.9	43.7±1.0	44.3±1.9
Galactose	7.5±0.2	10.5±0.2	10.0±0.4	10.8±0.8	10.2±0.1	11.0±0.5	9.9±0.5	10.1±0.8	9.9±0.5
A/X ratio	0.54	0.47	0.34	0.33	0.29	0.30	0.34	0.32	0.34

[a] Means ± standard error. A/X ratio = the ratio of arabinose to xylose. See Table 2.1 for abbreviations.

Table 2.3 Glycosidic linkage composition [mol%] of CAX hydrolyzates. [a]

Component	Linkage indicated	CAX	CH	$CAXH_1$	$CAXH_2$	$CHAX_1$	$CHAX_2$	$CHAXH_1$	$CHAXH_2$	CAXH-digest
2,3,5-Me_3-Ara	(Ara*f*)1→	15.3±0.4	8.9±0.6	7.8±0.2	6.4±0.5	5.1±0.2	4.8±0.4	5.8±0.3	4.1±0.4	5.8±0.3
3,5-Me_2-Ara	→2(Ara*f*)1→	3.5±0.5	5.0±0.3	5.5±0.3	5.5±0.2	6.3±0.4	6.0±0.2	6.5±0.2	6.4±0.3	6.5±0.2
2,5-Me_2-Ara	→3(Ara*f*)1→	3.6±0.2	4.5±0.2	9.1±0.2	10.0±0.4	8.8±0.7	9.0±0.3	9.5±0.6	9.9±1.0	12.5±0.6
2,3-Me_2-Ara	→5(Ara*f*)1→	1.4±0.6	3.2±0.1	3.5±0.1	3.9±0.1	4.0±0.6	4.3±0.5	5.0±0.3	4.7±0.2	5.0±0.3
2,3,4-Me_3-Xyl	(Xyl*p*)1→	22.9±2.1	23.3±0.9	19.7±1.2	18.9±0.6	19.9±1.1	19.5±0.9	20.3±1.9	18.8±0.3	20.3±1.9
2,3-Me_2-Xyl	→4(Xyl*p*)1→	11.9±0.7	14.9±1.1	16.7±0.4	19.4±0.3	18.5±1.0	21.2±1.8	15.8±0.8	17.4±0.6	10.8±0.8
2-Me_1-Xyl	→4(Xyl*p*)1→3↑	26.1±1.1	21.7±0.9	20.6±0.7	18.7±0.4	20.9±0.9	17.8±1.3	19.7±1.1	17.7±0.8	19.7±1.1
Xyl	→4(Xyl*p*)1→3↑↑2	11.9±0.5	13.0±0.2	10.0±0.4	10.2±0.6	10.3±0.2	10.0±0.6	13.2±0.9	12.8±0.7	15.2±0.9
2,3,4,6-Me_4-Gal	(Gal*p*)1→	3.4±0.1	5.5±0.2	5.9±0.5	6.1±0.3	5.4±0.1	5.7±0.4	5.4±0.6	5.1±0.4	5.4±0.6

[a] Values are expressed as a proportion of all partially methylated alditol acetates present. Ara = arabinose, Xyl = xylose, Man = mannose, Gal = galactose, Glu = glucose. See Table 2.1 for abbreviations.

Table 2.4 Solution viscosity of CAX hydrolyzates.

Sample	CAX	CH	$CAXH_1$	$CAXH_2$	$CHAX_1$	$CHAX_2$	$CHAXH_1$	$CHAXH_2$
Viscosity (cps)	3.7	3.4	1.3	1.4	1.0	1.0	1.5	1.3

See Table 2.1 for abbreviations.

Figures

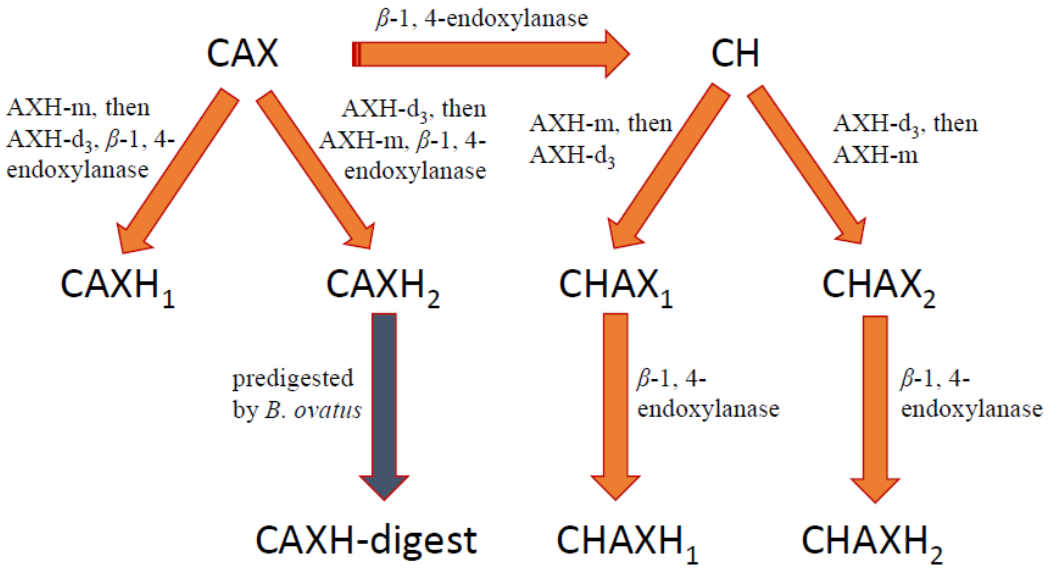

Figure 2.1 Preparation of CAX hydrolyzates using enzymatic and bacterial treatments.

See Table 2.1 for abbreviations.

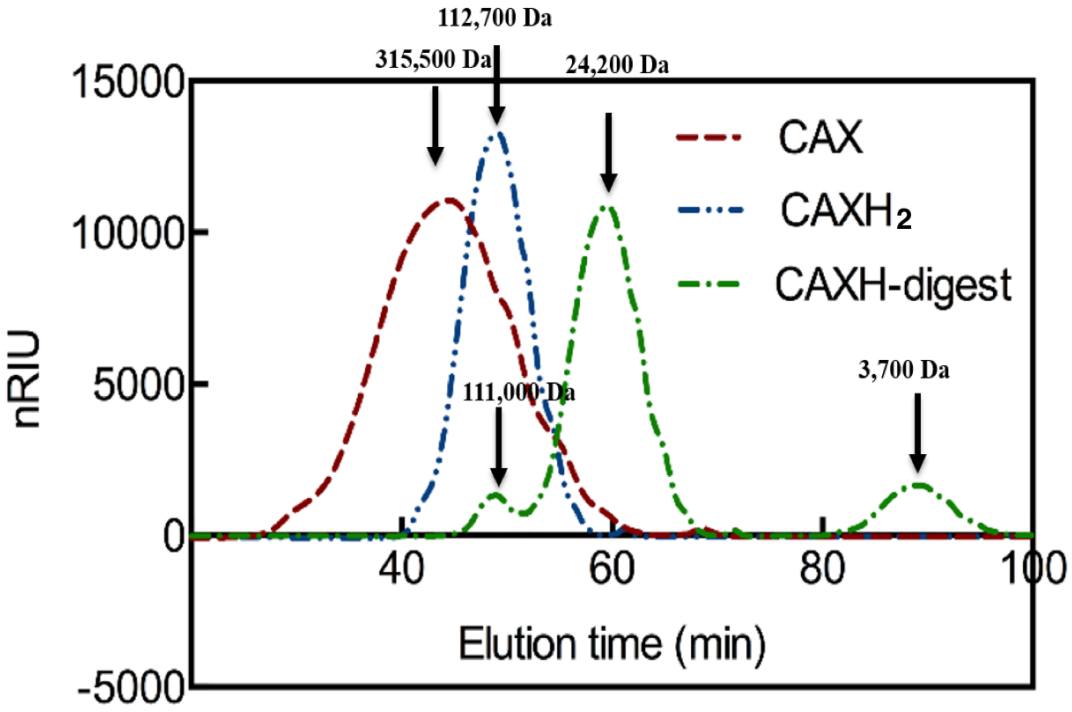

Figure 2.2 High performance size-exclusion chromatography elution profiles of arabinoxylan substrates: CAX (red), $CAXH_2$ (blue), and CAXH-digest (green). The average molecular weight of substrates shown in figure were calculated using pullulan standards as external standards.

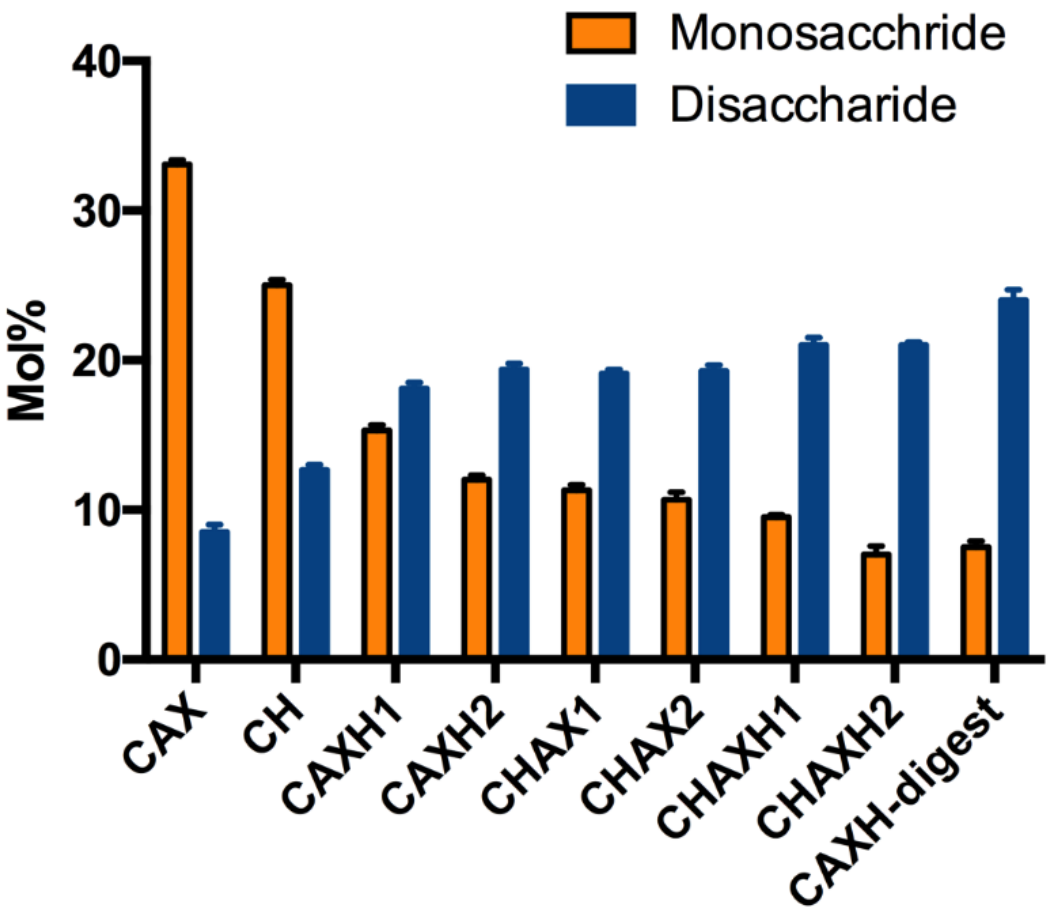

Figure 2.3 Distribution of branch length of CAX hydrolyzates.

See Table 2.1 for abbreviations.

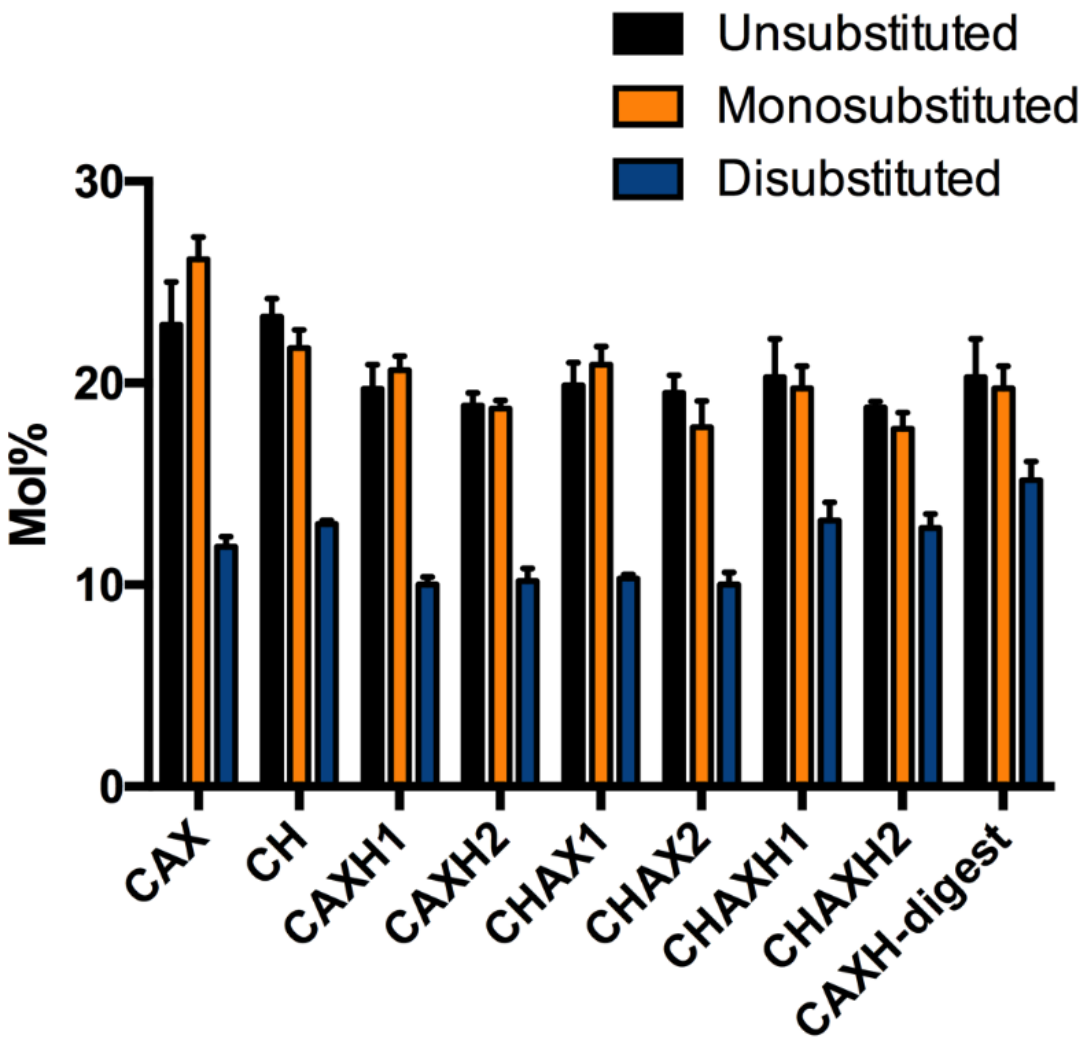

Figure 2.4 Substituent types in CAX hydrolyzates.

See Table 2.1 for abbreviations.

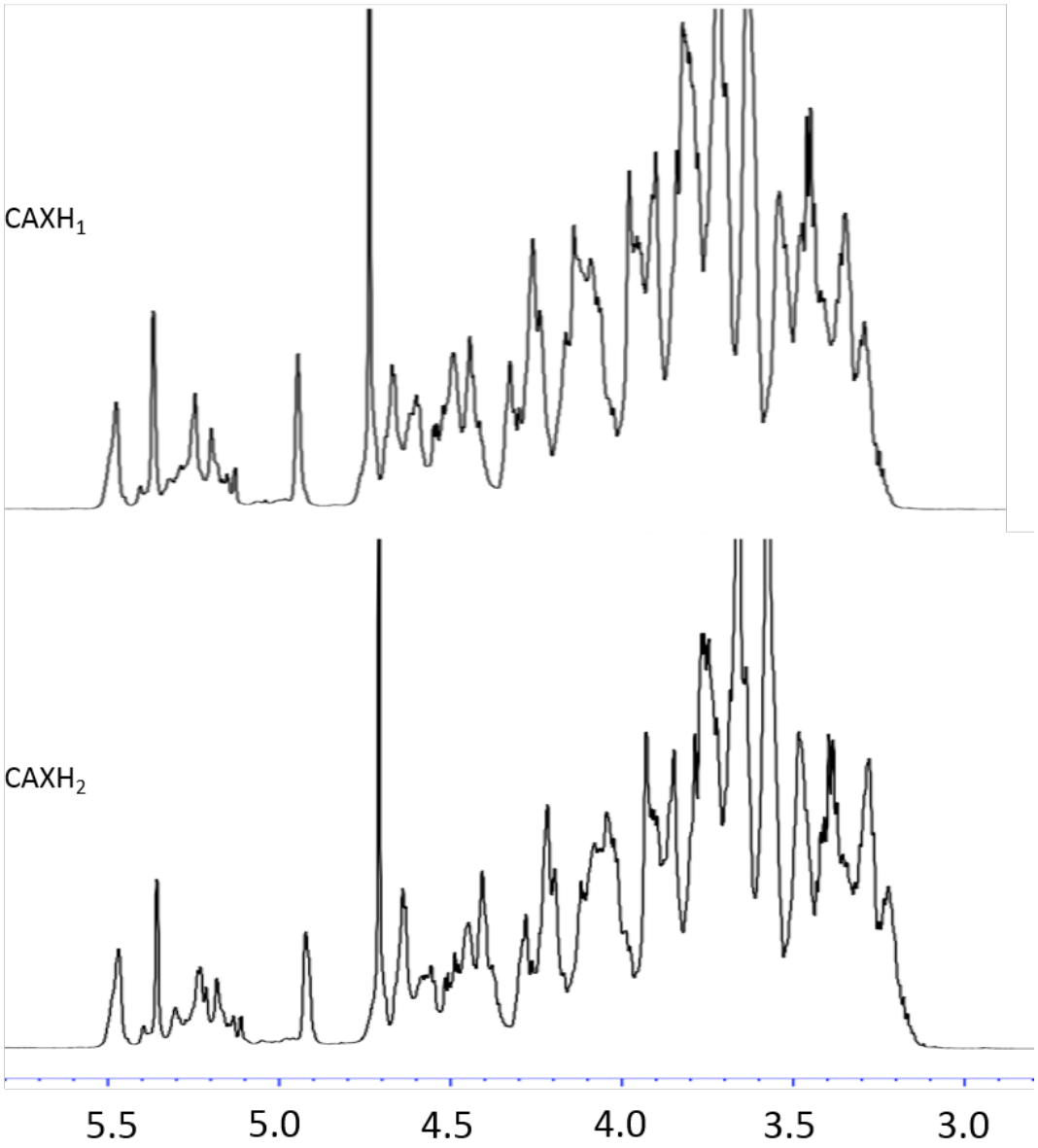

Figure 2.5 ^{1}H NMR (800.1 MHz) spectrum of $CAXH_1$ and $CAXH_2$ determined at 25 ºC. δ 4.46 ppm: the linkage of *β*-1, 2, 4-linked Xyl*p*, suggesting the 2-O substituted xylose units (Bendahou et al., 2007; Fischer et al., 2004; Yin et al., 2012); 5.30 and 5.23 ppm: anomeric protons of Ara*f* linked to O-3 and O-2 position on the same Xyl*p* backbone units (Hoffmann, Geijtenbeek, et al., 1992; Hoffmann, Kamerling, et al., 1992); δ 5.30

ppm: the combination of two arabinose disubstituents or one arabinose disubstituent neighboring to another single arabinose substituent (Hoffmann, Geijtenbeek, et al., 1992; Hoffmann, Kamerling, et al., 1992); δ 4.48 ppm, 4.46 ppm and 3.75 ppm: unsubstituted Xyl*p* connected with mono- or unsubstituted Xyl*p* (Hoffmann, Kamerling, et al., 1992). See Table 2.1 for abbreviations.

a

CAXH$_1$

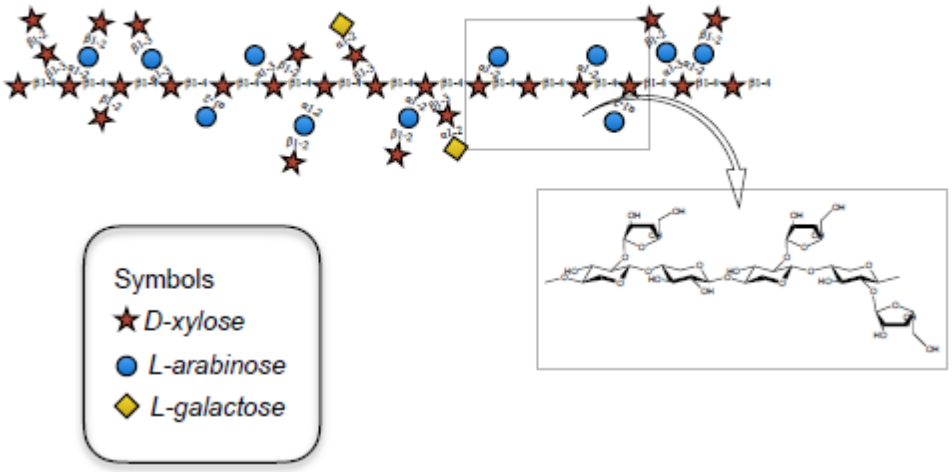

CAXH$_2$

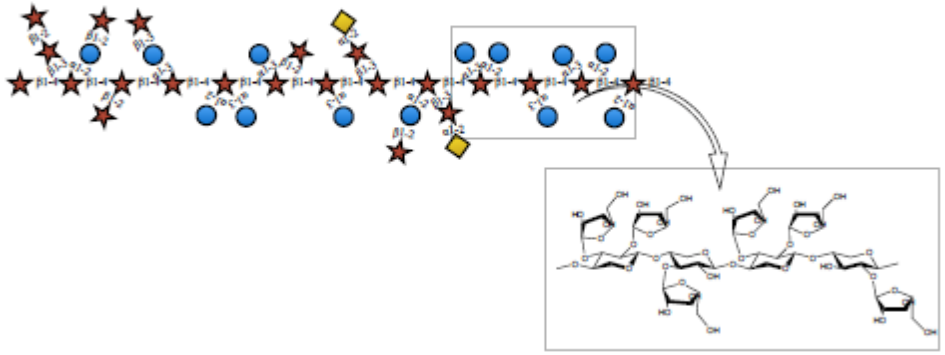

b

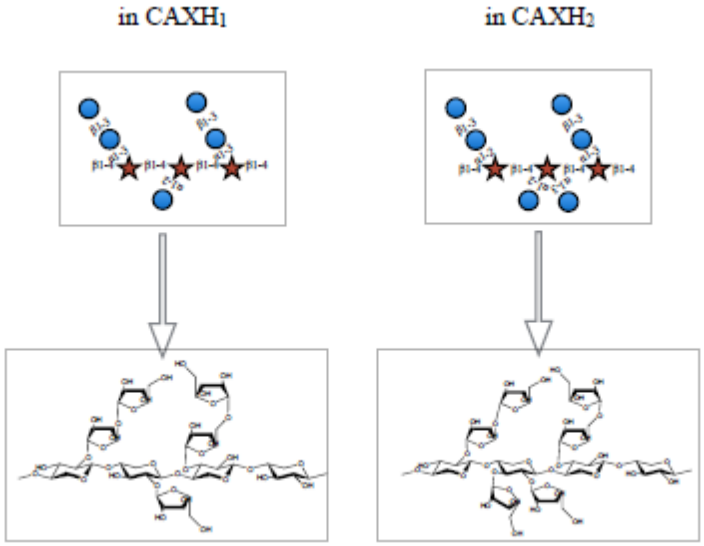

Figure 2.6 Models for the difference between $CAXH_1$ and $CAXH_2$.

a) Multiple arabinose branches in the same region. b) Arabinose branches in different regions between long branches. See Table 2.1 for abbreviations.

CHAPTER 3. CHANGE OF GUT BACTERIAL GROWTH DRIVEN BY SPECIFIC FIBER STRUCTURAL PATTERNS

3.1 Abstract

Understanding dietary fiber requirements for target gut bacterial growth is important for desired microbiota shifts. However, the connection between fiber structure and change of bacterial growth are still to be determined from dietary fiber perspective. Here, using corn bran arabinoxylan enzymatic hydrolyzates ("CAX hydrolyzates") as model structures, modified hydrolyzate structures with subtly changed arabinosyl branching structure were shown to significantly, and with high specificity, delay the lag phase of *Bacteroides xylanisolvens* XB1A (*B. xylanisolvens*) (up to 6 h), a common member of the gut microbiota. This, in turn, decreased the competitiveness of *B. xylanisolvens* in an artificial community additionally containing *Bacteroides ovatus* 3-1-23 (*B. ovatus*) and *Bacteroides cellulosyliticus* DSM 14838 (*B. cell*), resulting in notable suppression in growth of *B. xylanisolvens* in the model community. Further work showed that transcription of the arabinoxylan encoding polysaccharide utilization loci (PUL) of *B. xylanisolvens* adjusts to the change in CAX hydrolyzate structures. Together, our results show a high level of dependence of *Bacteroides* strains on structural features in dietary

fiber that was not known before, and support the hypothesis that specific dietary fiber structures can be identified to exert a selective response on members of the microbiota.

3.2 Introduction

Dietary fibers, which are in large part non-starch polysaccharides from the cell walls of cereal and legume grains, fruits and vegetables, are not degraded by human upper digestive tract and therefore serve as the major food source for gut microorganisms (DeVries et al., 1999). Dietary fiber consumption plays a significant role in modulating human health through maintaining our resident gut microbes against diet-related chronic diseases such as obesity, diabetes, inflammatory bowel diseases, and even colon cancer (Desai et al., 2016; Macfarlane, 2008). For instance, the promotion of butyrate-producing bacteria has been shown to be associated with the prevention of diabetes through the gut-brain interaction mechanism (De Vadder et al., 2014). A new view is that the health benefits of dietary fiber are dependent on target bacteria and that they can be stimulated (Desai et al., 2016). Thus, understanding of bacteria-specific degradation of dietary fibers will be required to understand the promotion (or suppression) of desired (undesired) gut bacteria. *Bacteroidetes* in gut utilize fiber structures involving gene clusters referred to as polysaccharide-utilization loci (PUL), which allow them to secrete proper enzymes, binding proteins, and transporters to degrade fibers with particular glyosidic linkages and use the resultant sugars for energy. Here, we use the dietary fiber termed arabinoxylan as a model fiber as it has a substantial complexity and variability of structure both within the polysaccharide and among polysaccharides from different botanical sources and regions.

A more detailed knowledge of dietary fiber structure and its specificity to PULs is important, but currently unknown, to identify whether and how proper fiber structures can control the growth behaviors of desired gut bacteria.

A perspective on fiber structure related to the gut bacteria is that there are discrete structures which correspond to gut bacterial PULs, suggesting the possibility of high specificity of fiber structure related to bacterial growth (Hamaker & Tuncil, 2014). Furthermore, work in our lab has shown that fiber structures influence competition relationships among bacteria, allowing us to think of the potential of using dietary fiber structures to modulate gut bacterial communities. Here we ask the questions, 1) how specific are PULs in different gut bacterial strains to carbohydrate structures, 2) do minor changes in structure change bacterial growth parameters, and 3) can specificity of structure be used to promote or suppress growth of a strain in a model competitive environment. It appears that the human gut microbiome can be easily damaged, with diversity declining and species disappearing because of lack of dietary fiber (Sonnenburg et al., 2016), or treatments such as misuse or overuse of antibiotics (Cho et al., 2012; Cox et al., 2014). Our challenge now is to find a novel, gut bacteria friendly strategy to achieve promotion (or suppression) of desired (undesired) gut bacteria.

Arabinoxylan (AX), a major component of many plant cell walls, is a commonly found dietary fiber in cereal-derived foods (Agger et al., 2010; Allerdings et al., 2006; Brett et al., 1996). The number, complexity, and density of the side chains on arabinoxylan make the structure varied. The current study was undertaken using this polysaccharide as a model for complex polysaccharide structures in general to investigate the impact of changes to structure on growth and competitiveness of a prominent human gut bacteria, *Bacteroides*

xylanisolvens, which utilizes xylan structures involving two distinct gene clusters (Despres et al., 2016).

In this study, we show that subtle modification of arabinosyl moieties attached to the xylose backbone and the structural forms of corn bran arabinoxylan enzymatic hydrolyzates (CAX hydrolyzates) are significant factors responsible for growth characteristics of *B. xylanisolvens* through a mechanism of adjustment of its xylan-related PUL. Furthermore, a suppression strategy for *B. xylan* was carried out due to a hypothesized decreased competitiveness of *B. xylanisolvens* resulting from a delay in its lag phase length. Together, the study demonstrates a high dependence of strains on fiber structural features for growth and establishes a suppression model for target gut bacteria using dietary fibers. This implies the potential to deliberately change target strains within the competitive environment of the human colonic microbiota using proper selection of dietary fibers.

3.3 Materials and Methods

3.3.1 Materials

3.3.1.1 Bacterial strains

B. ovatus 3-1-23, *B. cellulosyliticus* DSM 14838 and *B. xylanisolvens* XB1A were obtained from Dr. Eric C. Martens, Department of Microbiology & Immunology, University of Michigan Medical School, Ann Arbor, MI.

3.3.1.2 Corn arabinoxylan and enzymes

As shown in Chapter 2, dry-milled corn bran, particle size < 50 μm, was a gift from Bunge Milling (St. Louis, MO), and *α*-amylase from *Bacillus licheniformis*, protease from *Bacillus amyloliquefaciens* and other analytical chemicals purchased from Sigma; Multifect® AXH-d_3, AXH-m, endoxylanase gifts of Genencor International Inc., Rochester NY.

3.3.2 Methods

3.3.2.1 Extraction of corn arabinoxylan from corn bran and enzymatic modifications of corn arabinoxylan extracts

The procedures of extraction and enzymatic modifications of corn arabinoxylan polymers were described in Chapter 2 (2.3.2.1 and 2.3.2.2).

3.3.2.2 Bacterial culture and determination

Bacterial growth experiments were performed using *Bacteroides* strains *B. ovatus* 3-1-23, *B. cellulosyliticus* DSM 14838 and *B. xylanisolvens* XB1A in minimal medium (MM). Final concentration of all common components contained: 100 mM KH_2PO_4 (pH 7.2), 15 mM NaCl, 8.5 mM $(NH_4)_2SO_4$, 4 mM L-cysteine, 1.9 μM hematin/200μM L-histidine (prepared together as a 1,000x solution), 100 M $MgCl_2$, 1.4 M $FeSO_4 \cdot 7H_2O$, 50

M $CaCl_2$, 1 g ml^{-1} vitamin K_3, and 5 ng ml^{-1} vitamin B_{12}. Minimal medium was prepared at 10X concentration and sterilized by filtration (0.22 m pore size). Corn arabinoxylan polymers were added to MM at a final concentration of 0.5% (w/v) and were sterilized by autoclaving in distilled water at 1% (w/v). Medium was reduced by adding L-cysteine just before use and immediately placed into an anaerobic chamber (Coy Manufacturing, Grass Lake, MI), and then used within 3 h (Martens et al., 2008).

3.3.2.3 Gene transcriptional experiment

A transcriptional assay of bacteria was conducted. *B. xylanisolvens* was cultured in 5 ml of minimal media containing 0.5% (w/v) fiber substrates. Triplicate bacterial cultures were harvested at mid-lag phase and placed in RNAprotect (Qiagen), then stored at -80 °C overnight, before purification with RNeasy kit (Qiagen). RNA purity was assessed spectrophotometrically, and 1 mg of RNA was used immediately for reverse transcription (QuantiTect Reverse Transcription kit, Qiagen). Quantitative Real time PCR was performed in a 96-well plate on a Light Cycler 480 System (Roche) with Fast Start Essential DNA Green Master (Roche) using designed primers. Reactions were carried out in 10 ml, consisting of 20 ng of cDNA, and 0.125 mM (16 S rRNA) primer mix. Reaction conditions: 95 °C 600 s, followed by 45 cycles of 95 °C for 10 s, 55 °C for 10 s, 72 °C for 10 s. Cq values were calculated using Light Cycler 480 SW 1.5. Data were normalized to 16 S rRNA transcript levels, and change in expression level calculated as fold-change compared with minimal media, glucose cultures. Experiments were done in triplicate.

3.3.2.4 Mixed-culture of bacteria

Quantitative RT-PCR (qPCR) was conducted for the abundance of each strain in the community. After extraction of genomic DNA from bacterial strains using the Wizard Genomic DNA Purification Kit (Promega), DNA purity and concentration were determined and the number of copies was determined by qPCR. The qPCR was carried out in CFX 96 BioRad as follows: 2 min 30 s at 98 °C for initial activation of enzymes, 45 cycles of 5 s at 98°C, 10s at 58°C and 2 s at 72°C. Experiments were done in triplicate.

3.3.3 Statistical analyses

Statistical differences were determined using the Statistical Analysis System software package version 9.2 (SAS Institute, Cary, N.C., U.S.A.). Differences at each time point were analyzed using repeated analyses of variance, and differences between least square means were calculated using Fisher's least significant difference test. Substrate and time were fixed effects of the model and the latter was included as the repeated measurement.

3.4 Results and Discussion

3.4.1 CAX hydrolyzates with changes of arabinosyl moieties attached to xylan backbones

CAX hydrolyzates were prepared from alkali-extracted CAX, which is one of highly branched and structurally complex heteroxylans found in cereals (Rumpagaporn et al., 2015). Due to the treatment with alkali, the ester bonds of the crosslinks in arabinoxylan are broken which converts the fiber to a soluble form. CAX-hydrolyzates with subtly different structural transformations were prepared by selectively trimming arabinosyl branches and cleaving of the xylan backbone using enzyme treatments (Fig. 3.1, six were made and the chosen two are shown). Two types of enzymatic treatments were used on the arabinosyl moieties of the corn arabinoxylan hydrolyzate (CH, CAX after β-1, 4-xylanase hydrolysis only) which has a more dense and complex branched structure than the native CAX (Xu, 2012): 1) a sequential application of arabinofuranosidase-m (AXH-m) that randomly removes arabinose branches from the mono-substituted backbone unit followed by an arabinofuranosidase, AXH-d_3, that removes the 3-O position arabinose from the di-substituted xylose units on the backbone, thus resulting in a 2-O position arabinose branched structure; and 2) the opposite sequential application of AXH-d_3 to remove the 3-O position arabinose from the di-substituted backbone and then by AXH-m to remove arabinose branches from the mono-substituted backbone unit, to make a 2-O/3-O mixed and disubstituents arabinose branches on the xylan backbone as shown in Fig. 2.5. In chapter 2, we discussed the structural difference between these two fiber substrates (Fig.

3.1b), namely there are relatively open structural patterns of arabinosyl moieties in $CAXH_1$, while the arabinosyl patterns in $CAXH_2$ are relatively complex and closed. These differences were found only in part of the overall structure of hydrolyzates.

From the comparison of structural characterization of the eight different arabinoxylan-based substrates, CAX and CH displayed comparatively high A/X ratios (0.54 and 0.47) (Table 3.1). Glycosidic linkage analysis of CAX and CH (Table 3.2) showed that most of their arabinose arises from terminal substituted residues such as (Ara*f*) 1→ and (Xyl*p*) 1→ and fewer residues like →2 (Ara*f*) 1→ and →3 (Ara*f*) 1→, indicating that the percentage of disaccharide branches in large molecules like CAX and CH is relatively low and suggesting structures with long and narrow molecular shapes. In contrast, the other six CAX-hydrolyzates (Fig. 3.1a) have low A/X ratios but show high ratios of disaccharide branches with middle residuals like →2 (Ara*f*) 1→ and →3 (Ara*f*) 1→, and low terminal residues, indicating relatively short and broad structural forms.

Furthermore, all of six CAX hydrolyzates (Fig. 3.1a) shared similar neutral sugar composition (Table 3.1) with arabinose/xylose ratios around 0.30. However, differences were found in the fiber molecular forms, especially at the level of the arabinosyl side chains. Compared to $CAXH_1$, $CAXH_2$ had somewhat less terminal arabinose and xylose, slightly more residues like →3 (Ara*f*) 1→ (from 9.1% to 10.0%). $CHAX_1$ and $CHAX_2$ showed highest →4 (Xyl*p*) 1→ percentage (18.5 and 21.2%) indicating more unsubstituted regions in these two substrates, and suggesting somewhat more loose and accessible structures. $CHAXH_1$ and $CHAXH_2$ structures had abundant terminal (Xyl*p*) 1→ (20.3% and 18.8%) and disubstituted →4 (Xyl*p*) 1→3↑↑2 (13.2% and 12.8%) as well as low amount of

unsubstituted →4 (Xyl*p*) 1→ regions (15.8% and 17.4%), indicating that these substrates had the highest branch density among the structures of the six candidate substrates.

3.4.2 Bacterial growth on structurally different corn arabinoxylan substrates

Notable lag phase shift of B. xylanisolvens corresponding to structural changes of CAX hydrolyzates

Lag phase is defined as the preparation stage prior to growth of bacteria utilizing dietary fiber, referring to recognition, binding and transportation of carbon sources such as specific fiber structures (Rolfe et al., 2012). Notably, of the paired substrates ($CAXH_1$ vs. $CAXH_2$, $CHAX_1$ vs. $CHAX_2$, $CHAXH_1$ vs. $CHAXH_2$), as described above to have different branched structures on three different endoxylanase-treated base structures, $CAXH_1$ and $CHAXH_2$ caused substantially delayed lag phase and growth of *B. xylanisolvens*, even though the paired fiber substrates shared similar sugar compositions (Fig. 3.2a, f). Lag phase change was 6 h in the *B. xylanisolvens* pure culture between $CAXH_1$ and $CAXH_2$ (Fig. 3.2a, b). Despite the delayed lag phase, growth of the strain on the paired substrates was of similar rate and extent, suggesting that the differences in structural features of $CAXH_2$ and $CHAXH_2$ triggered *B. xylan*'s lag phase response at the recognition level. Growth profiles of *B. cell* and *B. ovatus* were obtained on $CAXH_1$ and $CAXH_2$ and neither showed change in lag phase, showing a strain-dependent effect (Fig. 3.2c, d).

A possible explanation for the above results is that the subtle change of the side chain arabinosyl patterns of the two substrates resulted in slower recognition for $CAXH_2$

and delay in gene transcription of *B. xylanisolvens* XB1A for the appropriate PUL for arabinoxylan. Perhaps less likely, in light of the retained ability of the strain to utilize $CAXH_2$ and $CHAXH_2$ is a reduced accessibility of fiber molecules to the enzyme and binding protein assembly (xylan utilization system) for digestion.

3.4.3 Gene expression during the lag phase of *B. xylanisolvens* XB1A

Transcription of xylan-receptor related gene regulated by CAX hydrolyzates structures

In order to further test the mechanism in metabolic change of *B. xylanisolvens* XB1A during the lag phase, Arabinoxylan-encoding PUL genes at the transcriptional level, related to xylooligosaccharide recognition, binding and reception, were determined by a time course of expression after exposure of *B. xylanisolvens*. BXY_29250 and BXY_46550 respectively represent xylooligosaccharide receptor proteins on bacterial outer membranes (Despres et al., 2016); while BXY_29570 represents the receptor proteins on inner membranes. *B. xylanisolvens* XB1A took nearly twice the time on $CAXH_2$ than $CAXH_1$ to express the related genes responsible for fiber receptor proteins, demonstrating that the delay in PUL transcriptional response of bacteria was due to specific CAX hydrolyzate structures (Fig. 3.1b). Transcriptional results mirrored delay in lag phase of *B. xylanisolvens* supporting the view that fiber structural patterns influenced the growth of *B. xylanisolvens* through gene regulation.

As mentioned above, changes in lag phase shifts of *B. xylanisolvens* depended on the type of structural changes of the CAX hydrolyzates. Although the paired arabinoxylan

structures were treated the same way using the two arabinofuranohydrylases, of the $CHAX_1$ and $CHAX_2$ samples were not then hydrolyzed by β-1, 4-endoxylanase; while $CHAXH_1$ and $CHAXH_2$ had the same treatment as $CAXH_1$ and $CAXH_2$ including the subsequent endoxylanase treatment (Fig. 1a). As a result, three groups with similar branch patterns were made: 1) Group 1, $CAXH_1$ and $CAXH_2$; 2) Group 2, $CHAX_1$ and $CHAX_2$; and 3) Group 3, $CHAXH_1$ and $CHAXH_2$. The possible explanation for the lack of significant delay in lag phase for $CHAX_2$ is that the Group 2 molecules have a loose-form with a higher degree of unsubstitution due to the lack of β-1, 4-endoxylanase treatment. Unsubstituted areas in $CHAX_1$ and $CHAX_2$ would be relatively easy to hydrolyze and sugar products could trigger transcriptional events that would contribute to the rapid growth curves for Group 2. In this case, the effect of the different arabinosyl side chain patterns would be weakened, because the bacteria would consume the xylan backbone first instead of digestion of the branched arabinosyl sections. In support of this structure-function argument, $CHAXH_2$ in Group 3 showed an even larger delay in lag phase than $CAXH_2$ of Group 1 that would be related causatively to the dense branched structures seen in the structural analysis related to the two-time endoxylanase treatments at different point of its preparation.

The CAX hydrolyzates studied appear to have two primary parts in their molecular structures: 1) the functional parts, the patterns of arabinosyl side chains responsible for the lag phase change of *B. xylanisolvens*; 2) the complementary parts, other parts of molecules that influence the effect of the functional parts. Arabinosyl side chain patterns in the CAX hydrolyzates serve as functional parts responsible for the lag phase change of *B. xylanisolvens*, while other parts acted as complementary parts with similar arabinosyl

branches respectively in Groups 2 and 3, such as loose areas with higher degree of unsubstitution in Group 2 reducing the lag phase change, and dense structures in Group 3 enhancing it.

3.4.4 In competitive environments, *B. xylanisolvens* was suppressed by CAX polymers with specific structural features

Gut microorganisms grow and develop at high density in the competitive distal intestinal ecosystem (Gerritsen et al., 2011; Rinttila & Apajalahti, 2013). There, hundreds of bacterial species coexist and interact with each other, and access carbohydrates through different competitive strategies for nutrients, some seemingly selfish (Cuskin et al., 2015) and others cooperative (Rakoff-Nahoum et al., 2016). The next experiment addressed the question whether the delay in lag phase of *B. xylanisolvens* caused by selected CAX hydrolyzates reduces its ability to compete in a model competitive gut bacteria consortium. From another perspective, we ask the question can manipulation of structural features of dietary fiber be used to alter competitiveness and growth of a gut bacteria?

An artificial community comprised of B. xylanisolvens, B. cellulosyliticus, and B. ovatus was made where all bacterial members are xylan degraders and B. cellulosyliticus showed stable hydrolysis capacity of CAX hydrolyzates. On the other hand, B. ovatus showed a notable alteration when fed by different structures; it grew poorly on complex structures like CAX, but grew strongly on relatively simple arabinoxylan structures such as wheat arabinoxylan or sorghum arabinoxylan (Xu, 2012). In the current study, the growth profile of each member of the community when fed CAX hydrolyzates was

recorded to investigate the performance of *B. xylanisolvens* on the fiber structures that delayed lag phase.

As shown in Fig. 3.4, decrease in *B. xylanisolvens* abundance in the artificial community was consistent with its delay in lag phase (Fig. 3.2a, f) induced by the CAX hydrolyzates $CAXH_2$ and $CHAXH_2$ (Fig. 3.4d, h). In response to the lag time change from 6 h on $CAXH_1$ to 12 h on $CAXH_2$ (Fig. 3.2a), the proportion of *B. xylanisolvens* decreased from 32.5% (Fig. 3.4b) to 18.2% (Fig. 3.4d). Compared to feeding on $CAXH_1$, abundance of *B. cell* on $CAXH_2$ increased from 31.3% to 43.1%, and of *B. ovatus* remained constant at 36.2% to 37.7%.

$CHAXH_1$ and $CHAXH_2$ are modifications to the structures of $CAXH_1$ and $CAXH_2$ into denser branched structures, and were both shown above to extend lag phase times with $CH\text{-}AXH_2$ being considerable longer to around 15 h (Fig. 3.2f). These substrates were used to test whether further suppression of *B. xylanisolvens* could be achieved in the artificial community. Unlike the CAXH results above, in this case both of the substrates ($CHAXH_1$ and $CHAXH_2$) caused suppression of *B. xylanisolvens* (to 6.8 and 11.5% of total abundance, respectively) with a corresponding large increase of *B. cell* (to 79.6 and 67.4% of total abundance, respectively), and additional suppression of *B. ovatus* (to 13.5 and 21.1% of total abundance, respectively) (Fig. 3.4f and h). This inferred that change in lag phase disfavored *B. xylanisolvens*, but the general change to a more complex arabinoxylan structure had greater impact on the artificial community by favoring *B. cell* which is known to grow well on such structures (Xu, 2012). Furthermore, *B. ovatus* either was also suppressed by its inability to grow well on the more complex arabinoxylan structure or, in a cross-feeding arrangement as explained below, it was suppressed along with the

suppression of *B. xylanisolvens*. These overall findings present a question as to whether fiber structures can be designed for suppression of a target bacteria.

3.5 Conclusions

A poorly predictable impact of dietary fibers on the gut microbiota is a handicap to achieve desired bacterial change for human health benefits. This study provides evidence of a specific connection between complex xylans (CAX hydrolyzates), which are commonly found in the human diet, and the lag phase period of the gut bacteria *B. xylanisolvens*. The results suggest that structural patterns in complex dietary fiber could regulate the target commensal bacteria members of the gut microbiota in a precise way, and one that expands the perception of the potential of fiber to manipulate the gut microbiota. The study shows that the lag phase shift of *B. xylanisolvens* can be modulated by subtle changes in structural patterns of arabinoxylan, specifically the arabinosyl side chain type and distribution in CAX hydrolyzate structures. Built on past knowledge in this area, this work further provides a practical and solid relationship between specific fiber structures and utilization by gut microbes. The work showed that the expression of CAX hydrolyzate utilization related genes in *B. xylanisolvens* mirrored the growth response to changes in structural features of the corn AX molecules. The findings pose the question of whether diet consumption of gut microorganisms can be better regulated than we previously thought.

The work suggests that, unlike prebiotics which are defined as the non-digestible food ingredients that can stimulate the growth or activity of limited gut bacteria to improve

host health (DeVries et al., 1999), structurally complex dietary fibers like CAX hydrolyzates can be used in a broader way to either stimulate or suppress target bacteria. In treatment against a pathogenic bacteria using traditional strategies such as antibiotics or other medicine treatment, dietary fiber therapy conceivably could also be effective and would be a healthier choice by avoiding impaired colon microbiota. For instance, *Clostridium difficile*, which is responsible for infectious diarrhea and even death, frequently bloom in patients because of the drug resistance or microbiota disorders from antibiotics overuse or misuse (Climo et al., 1998; Neu, 1992; Neu et al., 1992). Dietary fiber structures targeted to promote growth of its competitors or even to suppress its own growth, as demonstrated in our findings, could be a novel strategy to control growth of *Clostridium difficile*.

Our discovery that target gut bacteria might be regulated by subtly different complex dietary fibers like CAX hydrolyzates, has significant implications for diet-related microbiota manipulation. Here, seemingly subtle structural patterns of complex dietary fiber contributed to bacterial growth manipulation in a model system. This finding supports the idea that the gut microbiota can be adjusted by diet with designed complex dietary fiber components in a controlled and personalized manner.

3.6 References

Agger, J., et al. (2010). "enzymatic xylose release from pretreated corn bran arabinoxylan: differential effects of deacetylation and deferuloylation on insoluble and soluble substrate fractions." J Agric Food Chem **58**(10): 6141-6148.

Allerdings, E., et al. (2006). "Isolation and structural identification of complex feruloylated heteroxylan side-chains from maize bran." Phytochemistry **67**(12): 1276-1286.

Brett, R. L., et al. (1996). "The influence of loading levels, temperature and environment on fibre failure during the fatigue of a SiC fibre reinforced Ti-MMC." Int J Fatigue **18**(1): 1-8.

Cho, I., et al. (2012). "Antibiotics in early life alter the murine colonic microbiome and adiposity." Nature **488**(7413): 621

Climo, M. W., et al. (1998). "Hospital-wide restriction of clindamycin: Effect on the incidence of Clostridium difficile-associated diarrhea and cost." Ann Int Med **128**(12): 989.

Cox, G., et al. (2014). "An unusual class of anthracyclines potentiate Gram-positive antibiotics in intrinsically resistant Gram-negative bacteria." J Antimicrob Chemo **69**(7): 1844-1855.

Cuskin, F., et al. (2015). "Human gut Bacteroidetes can utilize yeast mannan through a selfish mechanism." Nature **517**(7533): 165-U186.

De Vadder, F., et al. (2014). "Microbiota-generated metabolites promote metabolic benefits via gut-brain neural circuits." Cell **156**(1-2): 84-96.

Desai, M. S., et al. (2016). "A dietary fiber-deprived gut microbiota degrades the colonic mucus barrier and enhances pathogen susceptibility." Cell **167**(5): 1339-1353 e1321.

Despres, J., et al. (2016). "Xylan degradation by the human gut *Bacteroides xylanisolvens XB1A* (T) involves two distinct gene clusters that are linked at the transcriptional level." BMC Genomics **17**.

DeVries, J. W., et al. (1999). "A historical perspective on defining dietary fiber." Cer Foods World **44**(5): 367-369.

Gerritsen, J., et al. (2011). "Intestinal microbiota in human health and disease: the impact of probiotics." Genes Nutr **6**(3): 209-240.

Hamaker, B. R. and Y. E. Tuncil (2014). "A perspective on the complexity of dietary fiber structures and their potential effect on the gut microbiota." J Mol Biol **426**(23): 3838-3850.

Macfarlane, G. (2008). "Existing knowledge of the human gut microbiota." J Pediatr Gastroenterol Nutr **46 Suppl 1**: E10.

Martens, E. C., et al. (2011). "Mucosal glycan foraging enhances fitness and transmission of a saccharolytic human gut bacterial symbiont." Cell Host Microbe, **4**(5), 447-457.

Neu, H. C. (1992). "The crisis in antibiotic-resistance." Science **257**(5073): 1064-1073.

Neu, H. C., et al. (1992). "Antibiotic-resistance - epidemiology and therapeutics." Diagn Microbiol Infect Dis, **15**(2), S53-S60.

Rakoff-Nahoum, S., et al. (2016). "The evolution of cooperation within the gut microbiota." Nature **533**(7602): 255

Rinttila, T. and J. Apajalahti (2013). "Intestinal microbiota and metabolites-Implications for broiler chicken health and performance." J Appl Poul Res **22**(3): 647-658.

Rolfe, M. D., et al. (2012). "Lag phase is a distinct growth phase that prepares bacteria for exponential growth and involves transient metal accumulation." J Bacteriol **194**(3): 686-701.

Rumpagaporn, P., et al. (2015). "Structural features of soluble cereal arabinoxylan fibers associated with a slow rate of in vitro fermentation by human fecal microbiota." Carbohyd Polym **130**: 191-197.

Sonnenburg, E. D., et al. (2016). "Diet-induced extinctions in the gut microbiota compound over generations." Nature **529**(7585): 212-U208.

Xu, H. (2012). "Influence of the structural complexity of cereal arabinoxylans on human fecal fermentation and their degradation mechanism by gut bacteria." Ph.D. thesis, Purdue University.

3.7 Tables and Figures

Tables

Table 3.1 Composition of corn arabinoxylan enzymatic hydrolyzates[a]

Constituent	CAX	CH	$CAXH_1$	$CAXH_2$	$CHAX_1$	$CHAX_2$	$CHAXH_1$	$CHAXH_2$
Arabinose	27.4±1.9	22.2±0.8	17.1±1.0	17.5±0.7	14.2±1.2	14.7±0.8	15.0±1.4	14.0±1.2
Xylose	51.2±3.0	47.6±4.4	50.2±2.9	52.9±1.8	48.2±2.1	49.1±1.7	44.3±1.9	43.7±1.0
Galactose	7.5±0.2	10.5±0.2	10.0±0.4	10.8±0.8	10.2±0.1	11.0±0.5	9.9±0.5	10.1±0.8
A/X ratio	0.54	0.47	0.34	0.33	0.29	0.30	0.34	0.32

[a] Means ± standard error. See Table 2.1 for abbreviations.

Table 3.2 Glycosidic linkage composition [mol%] of corn arabinoxylan hydrolyzates[a]

Component	Linkage indicated	CAX	CH	$CAXH_1$	$CAXH_2$	$CHAX_1$	$CHAX_2$	$CHAXH_1$	$CHAXH_2$
2,3,5-Me_3-Ara	(Ara*f*)1→	15.3±0.4	8.9±0.6	7.8±0.2	6.4±0.5	5.1±0.2	4.8±0.4	5.8±0.3	4.1±0.4
3,5-Me_2-Ara	→2(Ara*f*)1→	3.5±0.5	5.0±0.3	5.5±0.3	5.5±0.2	6.3±0.4	6.0±0.2	6.5±0.2	6.4±0.3
2,5-Me_2-Ara	→3(Ara*f*)1→	3.6±0.2	4.5±0.2	9.1±0.2	10.0±0.4	8.8±0.7	9.0±0.3	9.5±0.6	9.9±1.0
2,3-Me_2-Ara	→5(Ara*f*)1→	1.4±0.6	3.2±0.1	3.5±0.1	3.9±0.1	4.0±0.6	4.3±0.5	5.0±0.3	4.7±0.2
2,3,4-Me_3-Xyl	(Xyl*p*)1→	22.9±2.1	23.3±0.9	19.7±1.2	18.9±0.6	19.9±1.1	19.5±0.9	20.3±1.9	18.8±0.3
2,3-Me_2-Xyl	→4(Xyl*p*)1→	11.9±0.7	14.9±1.1	16.7±0.4	19.4±0.3	18.5±1.0	21.2±1.8	15.8±0.8	17.4±0.6
2-Me_1-Xyl	→4(Xyl*p*)1→3↑	26.1±1.1	21.7±0.9	20.6±0.7	18.7±0.4	20.9±0.9	17.8±1.3	19.7±1.1	17.7±0.8
Xyl	→4(Xyl*p*)1→3↑↑2	11.9±0.5	13.0±0.2	10.0±0.4	10.2±0.6	10.3±0.2	10.0±0.6	13.2±0.9	12.8±0.7
2,3,4,6-Me_4-Gal	(Gal*p*)1→	3.4±0.1	5.5±0.2	5.9±0.5	6.1±0.3	5.4±0.1	5.7±0.4	5.4±0.6	5.1±0.4

[a] Values are expressed as a proportion of all partially methylated alditol acetates present. See Table 2.1 for abbreviations.

Figures

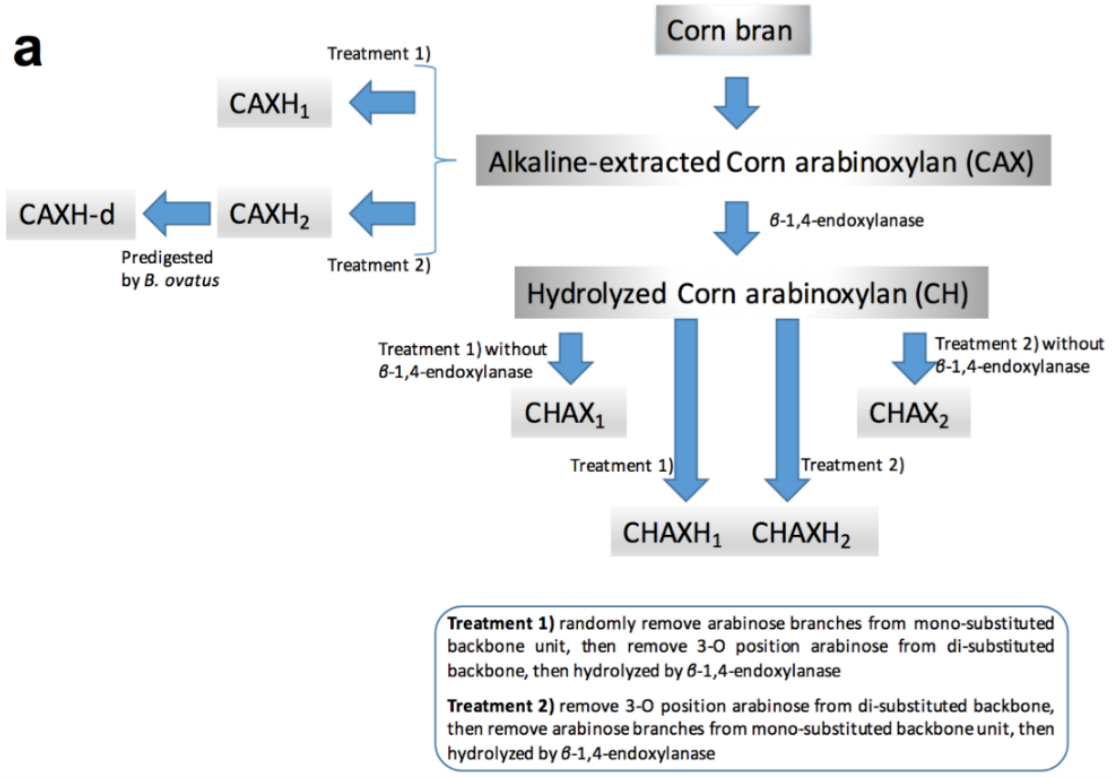
a
Corn bran
Treatment 1)
CAXH1
Alkaline-extracted Corn arabinoxylan (CAX)
CAXH-d
CAXH2
β-1,4-endoxylanase
Predigested by B. ovatus
Treatment 2)
Hydrolyzed Corn arabinoxylan (CH)
Treatment 1) without β-1,4-endoxylanase
Treatment 2) without β-1,4-endoxylanase
CHAX1
CHAX2
Treatment 1)
Treatment 2)
CHAXH1 CHAXH2
Treatment 1) randomly remove arabinose branches from mono-substituted backbone unit, then remove 3-O position arabinose from di-substituted backbone, then hydrolyzed by β-1,4-endoxylanase
Treatment 2) remove 3-O position arabinose from di-substituted backbone, then remove arabinose branches from mono-substituted backbone unit, then hydrolyzed by β-1,4-endoxylanase

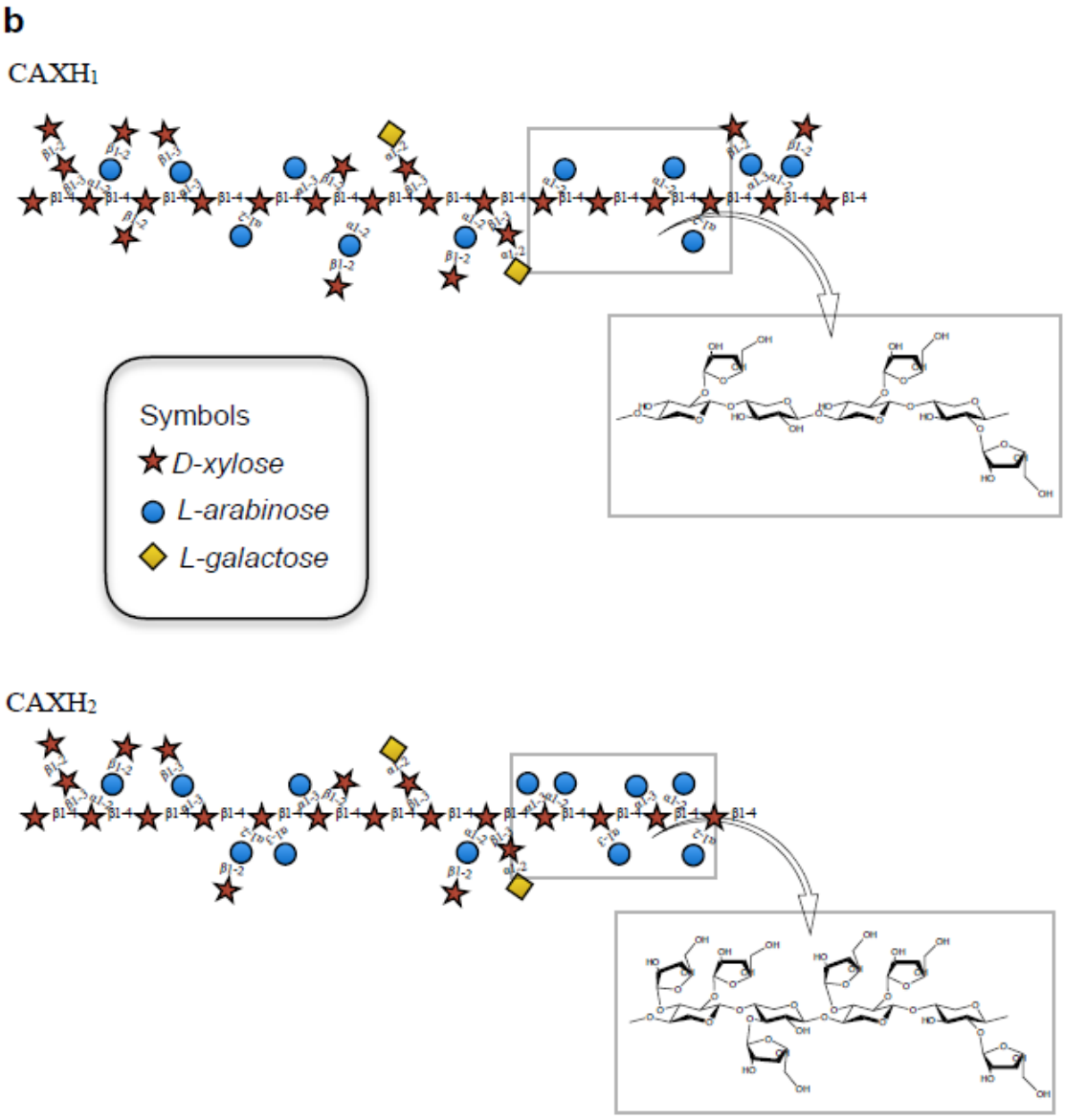

Figure 3.1 Flow chart for CAX hydrolyzates production and proposed structures for $CAXH_1$ and $CAXH_2$.

a) Production of CAX hydrolyzates from corn bran by treatment 1) and 2). b) Proposed structures of $CAXH_1$ and $CAXH_2$, showing the subtle difference on arabinosyl forms as branches after the two treatments. See Table 2.1 for abbreviations.

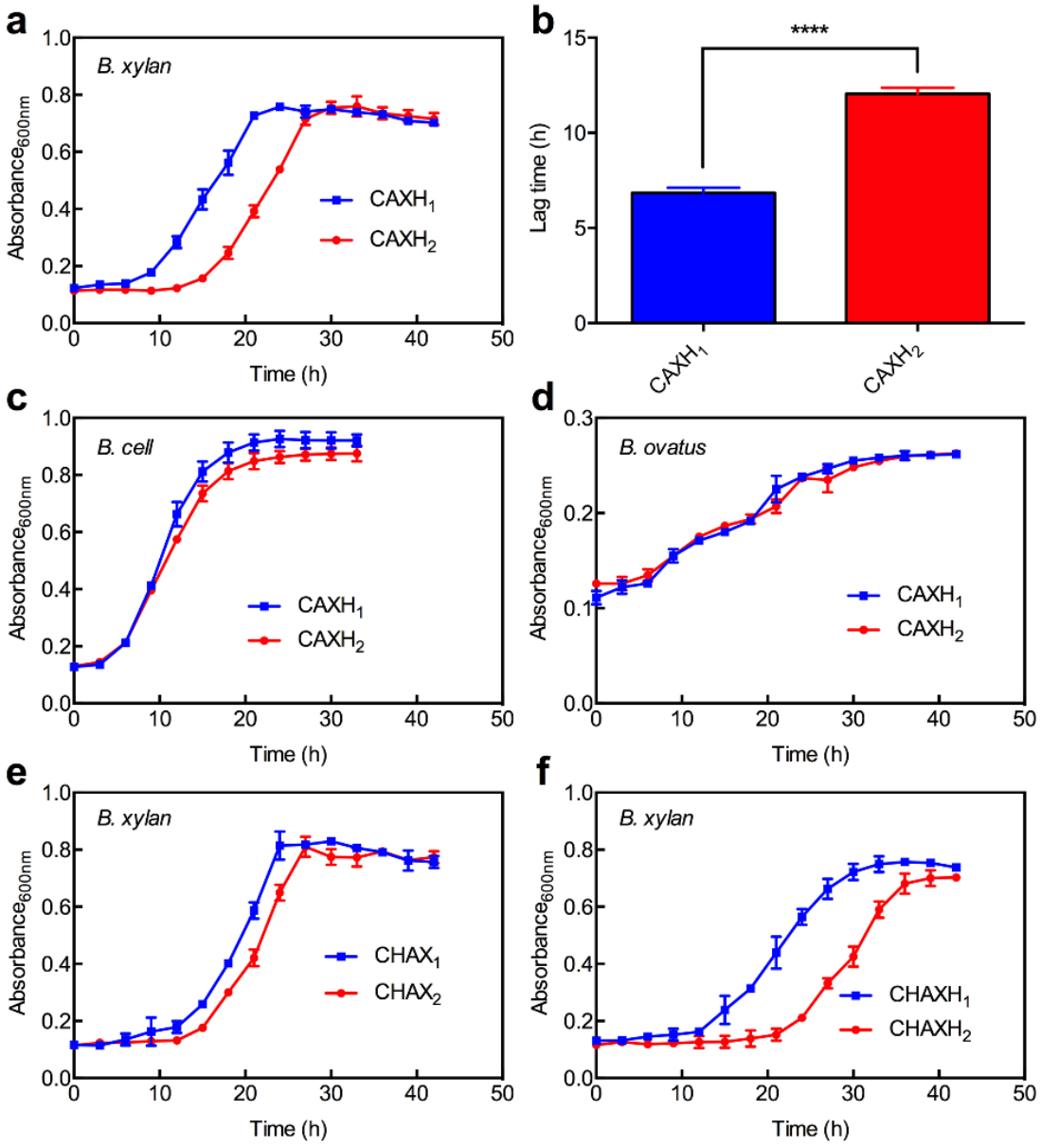

Figure 3.2 Growth of *B. ovatus*, *B. cellulosyliticus* and *B. xylanisolvens* on arabinoxylan substrates.

a) Absorbance curves for *B. xylanisolvens* in pure culture on $CAXH_1$ and $CAXH_2$, showing the notable shift in its lag phases. b) Statistical analysis of comparison between

two lag times of growth curves in a). c) Absorbance curves for *B. cellulosyliticus* in pure culture with similar lag phases. d) Absorbance curves for *B. ovatus* in pure culture on two substrates, showing a low capacity on CAX hydrolyzates digestion. e) Absorbance curves for *B. xylanisolvens* in pure culture on $CHAX_1$ and $CHAX_2$, showing relatively small shift of the lag phases. f) Absorbance curves for *B. xylanisolvens* in pure culture on $CHAXH_1$ and $CHAXH_2$, showing a large shift of its lag phases. See Table 2.1 for abbreviations.

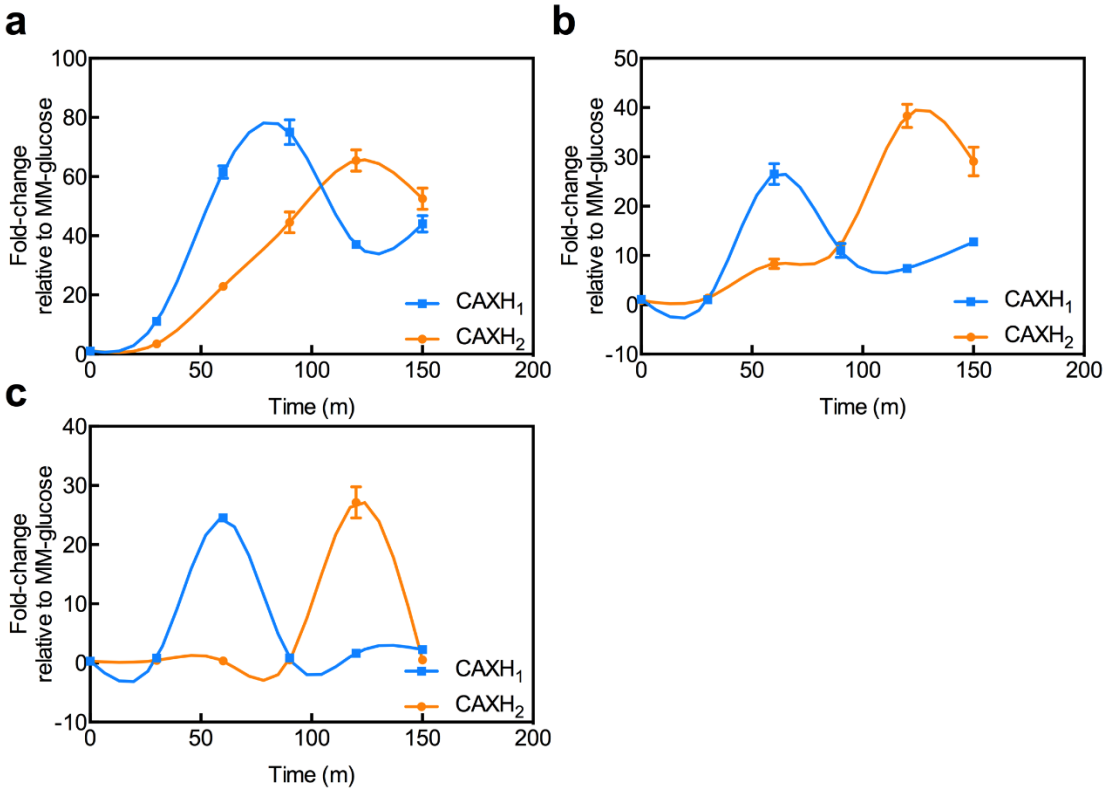

Figure 3.3 Gene transcription of PULs responsible for arabinoxylan degradation of *B. xylanisolvens*.

a) Transcriptional curves of gene BXY_29250, outer membrane TonB-dependent Receptor/SusC homolog, on $CAXH_1$ (light blue) and $CAXH_2$ (orange). b) Transcriptional profile of gene BXY_29270 on $CAXH_1$ (light blue) and $CAXH_2$ (orange) as TonB-dependent Receptor/SusC homolog. c) Another gene BXY_49550 transcriptional curves for xylooligosaccharides transporter on $CAXH_1$ (light blue) and $CAXH_2$ (orange). See Table 2.1 for abbreviations.

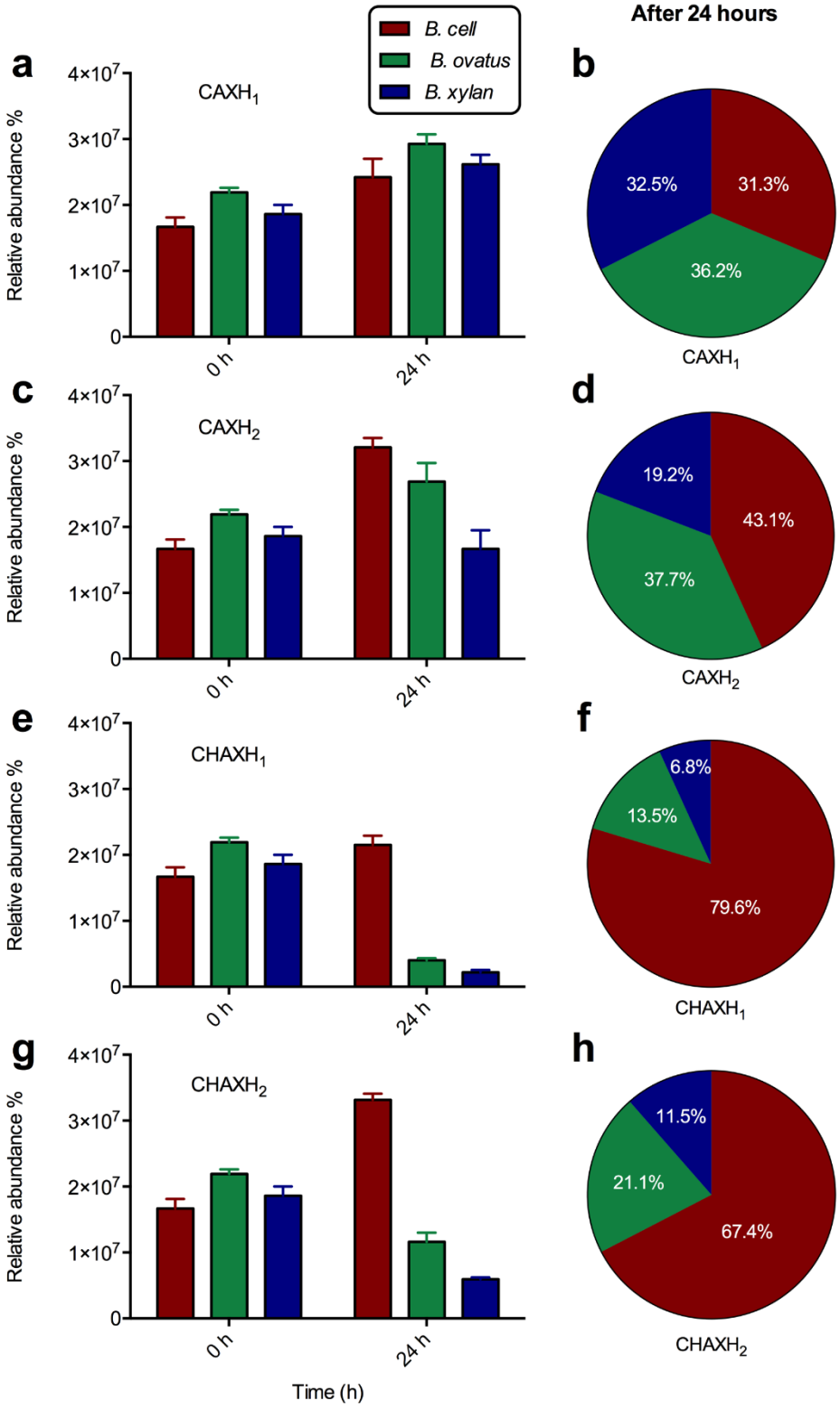
a
b
c
d
e
f
g
h
B. cell
B. ovatus
B. xylan
After 24 hours
Relative abundance %
4×10^7
3×10^7
2×10^7
1×10^7
0
CAXH1
CAXH2
CHAXH1
CHAXH2
0 h
24 h
Time (h)
32.5%
31.3%
36.2%
19.2%
43.1%
37.7%
6.8%
13.5%
79.6%
11.5%
21.1%
67.4%

Figure 3.4 Substrate induced change of microbial compositions in an artificial competitive community.

a) Growth change of strains on $CAXH_1$ after 24 h. b) Proportion of strain after 24 hours on $CAXH_1$. c) Growth change of strains on $CAXH_2$ after 24 h. d) Proportion of strain after 24 hours on $CAXH_2$. e) Growth change of strains on $CHAXH_1$ after 24 h. f) Proportion of strain after 24 hours on $CHAXH_1$. g) Growth change of strains on $CHAXH_2$ after 24 h. h) Proportion of strain after 24 hours on $CHAXH_2$. See Table 2.1 for abbreviations.

CHAPTER 4. STRUCTURAL FEATURES OF A CORN ARABINOXYLAN MODEL AFFECT ABILITY OF BACTERIA TO SURVIVE AND THRIVE IN A COMPETITIVE ENVIRONMENT

4.1 Abstract

Knowledge of interactions among bacteria in the gut microbial community relative to their access to food is crucial for an understanding of how predictable changes may be made in microbiota composition. Much is not clear regarding how dietary fiber structures impact nutritional interactions of gut bacteria in a particular community. Here, using an artificial microbial community, different arabinoxylan-based structures were used to create different competitive environments containing three xylan-utilizing *Bacteroides* strains. By cooperating with *Bacteroides xylanisolvens* XB1A (*B. xylanisolvens*), *Bacteroides ovatus* 3-1-23 (*B. ovatus*) was shown to survive by cross-feeding on a complex fiber structures that it cannot digest by itself. However, when on relatively simple arabinoxylan-based substrates, such cross-feeding cooperation between the two bacteria was not observed, indicating that cross-feeding cooperation is determined by fiber structure. High percentage of disubstituted xylose residues were determined as the key structural feature for suppressing *B. ovatus* utilization of corn arabinoxylan hydrolysates. In addition, long and complex branches (disaccharide) were indicated to obstruct hydrolysis by isolated

enzymes but not *B. ovatus*. *B. cellulosyliticus* DSM 14838 (*B. cell*) showed capacity to digest simple and complex xylan structures alone. On complex structure*, B. cell* is a strong competitor. While on simple structure, other bacteria like *B. ovatus* have ability to compete with *B. cell*. This study indicates manipulation of dietary fiber structures could be a promising approach to achieve desired gut microbiota compositions for personalized human health.

4.2 Introduction

The human distal gut harbors trillions of microbes whose composition and interactions are tightly associated with colon health (Qin et al., 2010). Accumulated evidence showed that compositional shifts of gut microbiota play a significant role in many chronic non-communicable diseases (Ley et al., 2005; Ley et al., 2006; Macfarlane et al., 2008; Sartor, 2008). For instance, the proportion of butyrate-producing bacteria in diabetic individuals is lower than healthy people (De Vadder et al., 2014).

Dietary fiber has been used as one of several strategies to manipulate the gut microbiota. Bacteria apply specific gene systems, PULs, to utilized different kind of fibers (Martens et al., 2009). It is reported that *B. ovatus* has different polysaccharide utilization loci for arabinoxylan with different complexities to make sure it can grow on different structures (Rogowski et al., 2015). This kind of specificity to structure, coupled with an idea that discrete structures of dietary fibers, both within and among polysaccharide classes, may be aligned to to encoded gene clusters in bacterial genomes (Hamaker & Tuncil, 2014), suggests that dietary fiber composition could be used to make fairly specific changes to the

gut microbiota for health-related purposes. However, it is still difficult to know the effects and efficiency of dietary fiber interventions on gut bacterial changes, and fundamental information is needed to know how fibers influence the but microbial community.

Bacteria coexist in anaerobic gut environments with other microorganisms and form communities in which they compete as well as form cooperative arrangements to access nutrients (Qin et al., 2010). Recent research (Benomar et al., 2015) shows that the exchange of cell molecules, including proteins, allowed the strain *D. vulgaris* to grow under the shortage of nutrients, indicating one of the possible mechanisms for bacteria cooperation. However, the knowledge of the effect of specific dietary fiber on the complex interactions that occur in bacterial consortia and how fiber structures form the basis for these interactions, is limited.

This study was undertaken using model corn arabinoxylan hydrolysates, to represent complex polysaccharide structures in general, to investigate the impact of defined fiber structures on growth and interactions of prominent human gut bacteria, *Bacteroides ovatus, Bacteroides xylanisolvens,* and *Bacteroides cellulosilyticus,* which all have high xylan-utilizing activity (Chassard et al., 2008; McNulty et al., 2013; Mirande et al., 2010; Whitehead & Hespell, 1990). The results provide information regarding strategies of bacterial members for survival and growth in competitive communities.

4.3 Materials and methods

4.3.1 Materials

As shown in previous chapters, in this study, dry-milled corn bran (particle size < 50 μm) was obtained from Bunge Milling (Danville, IL). Multifect® CX XL endoxylanase (445 XAU/mL) was from Genencor International Inc. (Rochester, NY). Arabinoxylan arabinofuranohydrolase AXH-d_3 and AXH-m were gifts from Novozymes North America Inc. (Franklinton, NC). Preparations of the Novozyme arabinofuranosidases were reported by Michlmayr et al. (Michlmayr et al., 2013). AXH-d_3 is a glycoside hydrolase (GH) family 43 enzyme cloned from *Humicola insolens* that selectively hydrolyzes the (1→3)-α-L-arabinofuranosyl residues of doubly substituted xylopyranosyl residues in the AXs. AXH-m is the GH51 enzyme cloned from *Meripilus giganteus* that catalyzes the removal of both (1→2) and (1→3)-α-L-arabinofuranosyl residues from singly substituted xylopyranosyl residues in the AXs. Other enzymes and chemicals were purchased from Sigma-Aldrich Co. (St. Louis, MO).

Isolated gut bacteria strains, *B. ovatus* 3-1-23, *B. cellulosyliticus* DSM 14838 and *B. xylanisolvens* XB1A were from Dr. Eric C. Martens, Department of Microbiology & Immunology, University of Michigan Medical School, Ann Arbor, MI.

4.3.2 Preparation of corn arabinoxylan substrates

4.3.2.1 Corn arabinoxylan extraction and hydrolysis

CAX was extracted as described in Chapter 2 (2.3.2.1). Debranched hydrolyzed corn AXs (CAXHs) were obtained using the method in Chapter 2 (2.3.2.2).

4.3.2.2 Predigest by *B. ovatus*

$CAXH_2$ (1g) was fermented by *B. ovatus* 3-1-23 in anaerobic chamber for 3 days. Supernatant was collected by centrifugation at 1000 *g*, as described in Chapter 2.

4.3.3 Structural analysis of corn arabinoxylan hydrolyzates

4.3.3.1 Molecular size by high performance size exclusive chromatography

Molecular size distributions were obtained using a HPSEC system consisting of a pump (Varian 9012, Varian Associates Inc., Walnut Creek, CA), a syringe sample loading injector (model 7125, Rheodyne Inc., Oak Harbor, WA) with a 100 µL sample loop, two columns with Superdex 30 and 200 analytical grade media (separation range Mw= $< 1 \times 10^4$ and 1×10^4 to 6×10^5, respectively) (Amersham Biosciences, Piscataway, NJ), and a refractive index detector (Varian star 9040, Varian Associates Inc., Walnut Creek, CA). Sample solutions (1% w/v) were prepared and injected (300 µl); deionized water with 0.02%

sodium azide was used as the eluent (flow rate of 0.4 ml/min). Data were collected with Varian's Star Chromatography Workstation (Version 4.51, Varian Associates Inc., Walnut Creek, CA). The retention times of pullulan standards (Polymer Laboratories, Santa Clara, CA) were used as external standards.

4.3.3.2 Monosaccharide composition analysis

Monosaccharide composition was obtained by the neutral sugar analysis method in AACC International Official Method 32-25 (AACC, 2000), using a smaller sample size (50 mg). Alditol acetates in ethyl acetate were quantified by gas chromatography using a capillary column SP-2330 (SUPELCO, Bellefonte, PA) with the following conditions: injector volume, 2 µl; injector temperature, 240 ºC; detector temperature, 300 ºC; carrier gas (helium), velocity 1.9 meter/second; split ratio, 1:2; temperature program was 160 ºC for 6 min, then 4 ºC/min to 220 ºC for 4 min, then 3 ºC/min to 240 ºC for 5 min, and then 11 ºC/min to 255 ºC for 5 min.

4.3.3.3 Glycosidic linkage characterization

Linkage analysis was performed by the method of Carpita and Shea (Carpita et al., 1989) with modifications: dried samples (3 mg) were dissolved in anhydrous DMSO (300 µl), and methylated. The methylated samples were hydrolyzed using 250 µl of 2 N trifluoroaceticacid (121 ºC for 1 h). The hydrolyzed samples were dissolved in 100 µl of 1M ammonium hydroxide, and 500 µl of DMSO containing 20 mg/ml of sodium

borodeuteride was added to reduce the aldyhyde groups. The mixture was incubated at 40 ºC for 90 min and 6-9 drops of glacial acetic acid were added and mixed to stop reduction reaction. 1-Methylimidazole (100 µl) and acetic anhydride (500 µl) were added for acetylation. Partially methylated alditol acetates in acetone were quantified by GC-FID-MS (7890A-5975C MSD, Agilent Technologies, Inc., Santa Clara, CA, USA) using a SP-2330 capillary column (injector volume, 1 µl; injector temperature, 240 ºC; detector temperature, 300 ºC; carrier gas, helium: 1.9 meter/second; split ratio, 100:1; temperature program, 100 ºC for 2 min, 8 ºC/min to 240 ºC for 20 min).

4.3.4 Bacterial growth experiment

4.3.4.1 Bacteria culture and determinations

The "*Bacteroides* minimal medium (as described in previous chapters)" was pre-inoculated with each bacterial strain: 1 ml of bacterial inoculum preparation was pipetted into a 1.5 ml centrifuge tube and was centrifuged at 7.2×1000 *g* for 1 min. The supernatant was discarded. Minimal medium (1 ml) was added and re-mixed with the bacterial pellet. The centrifuge step was repeated once for washing purpose. The washed bacterial pellet was re-suspended with 1 ml of minimal medium. Then, 500 µl of pre-inoculated minimal medium was diluted into 25 ml. Diluted bacterial inoculum (100 µl) was then inoculated into the prepared plates with 100 µl of substrate solution in each well. The plates were incubated in an anaerobic chamber for about 40 h at 37 °C. The bacterial growth was monitored by reading the turbidity at OD_{600}.

4.3.4.2 Growth profiles in multi-bacteria system

The mixture of two or three strains, bacteria in a 1:1 or 1:1:1 ratio (v/v). was incubated with the four substrates described above. Each culture (100 µl) was inoculated into another 100 µl of fresh substrate solution every day. Four days of incubation were conducted and samples were harvested at Day 1 and Day 4. DNA samples were extracted and purified using DNeasy Blood and Tissue Kit (Qiagen, Valencia, CA) according to the manufacturer's instructions. DNA concentration was determined by qPCR. Negative controls were conducted using the specific probe for one strain to detect the other two strains. Experiments were done in triplicate.

4.4 Results and discussion

4.4.1 Corn arabinoxylan substrates induce different growth profiles of gut bacteria

In this study, solubilized and isolated corn arabinoxylan (CAX) was structurally modified through use of debranching enzymes applied to remove the arabinosyl residuals from xylose backbones, endoxylanase to hydrolyze unsubstituted regions, and through treatment of substrates directly with a xylan-degrading bacteria. As described in Chapter 2 and 3, AXH-d_3 remove the 3-O terminal arabinosyl substituents from disubstituted xylose units and AXH-m removes the single arabinosyl residuals from monosubstituted xylose to produce a relatively loose structure. Endoxylanase hydrolyzes the xylose backbone from sparsely branched regions in the molecules. After treatment with the three enzymes, the

hydrolyzate $CAXH_2$, was collected and used for the next step (Fig. 4.1a). *Bacteroides ovatus*, a xylan-digesting gut bacteria member, which had shown poor ability to hydrolyze $CAXH_2$ (Fig. 4.1b), was used to further digest it to create an arabinoxylan hydrolyzate that it would be unable to grow on (termed as CAXH-digest).

4.4.2 *B. ovatus* survives on CAXH-digest with the help of another xylan-degrading gut bacteria member

Gut bacteria coexist in the human colon and appear to interact and communicate with each other to survive in different stressed environments (Canny & McCormick, 2008; Macpherson & Harris, 2004). When microbes are fed nutrients that they cannot digest by themselves, one of the possible strategies for the target bacteria is to cooperate with the members who can help them hydrolyze the substrates or produce the nutrients that the target bacteria can utilize (Germerodt et al., 2016; Seth & Taga, 2014). This is termed "cross-feeding", and involved a primary degrader to provide substrate for a secondary degrader. In the current study, three common gut xylan-digesting bacteria *B. ovatus* 3-1-23, *B. xylanisolvens* XB1A, and *B. cellulosilyticus* DSM 14838 were used to understand relationships and strategies bacteria use relative to glycan structures they can either easily utilize, or utilize with some difficulty, or cannot utilize. Different from *B. ovatus*, which could only partially use $CAXH_2$ and not use at all CAXH-digest, the other two *Bacteriodes* strains were good at utilizing complex xylan structures such as $CAXH_2$ and also grew on CAXH-digest (Fig. 4.2). For the growth of *B. xylanisolvens* and *B. cell*, CAX was a good substrate to utilize. For *B. xylanisolvens*, it utilized the more complex $CAXH_2$ structure

well, but with a longer lag phase (from 7 to 13 h) compared to growth on CAX. *B. cell* utilized $CAXH_2$ nearly as well as CAX with only a small lag in growth rate. The growth of these two bacteria on CAXH-digest decreased dramatically, however both bacteria could still grow, with a higher growth for *B. cell* (unlike *B. ovatus* which did not grow at all on CAXH-digest) (Fig. 4.1b). Therefore, CAXH-digest substrate was used, with the other substrates, to investigate the role of structure on cross-feeding. A competitive artificial community model was made by mixing different combinations of the three bacteria together.

Interestingly, as shown in Fig. 4.3, *B. ovatus* did not grow at all on CAXH-digest in the presence of *B. cell* (Fig. 4.3a), but regained the ability to grow when combined with *B. xylan* (Fig. 4.3b), indicating that either 1) *B. cell* completely utilizes the complex CAXH-digest substrate and leaves nothing for *B. ovatus* or that that digested parts freed by *B. cell* are still too complex for *B. ovatus* to use. *B. xylanisolvens* probably helped *B. ovatus* to overcome the block to its growth of a high proportion of disubstituted xylose side chains, according to the discussion below on the structure of CAXH-digest, and thus helping *B. ovatus* survive in the artificial community competitive environment. However, another reason for the cooperation between *B. xylanisolvens* and *B. ovatus* could be that the former simply releases more digested substrate for *B. ovatus* to utilize compared to *B. cell*. Although *B. cell* dominated growth in the community on the CAXH-digest substrate, *B. ovatus* and *B. xylanisolvens* maintained themselves at 30 h of incubation (Fig. 4.3b). As a result, *B. cell*'s overall growth decreased compared to the pure culture (Fig. 4.2b) or co-culture with *B. ovatus* (Fig. 4.3a).

4.4.3 The cross-feeding function of gut bacteria is substrate-structure dependent

When CAX and $CAXH_2$ served as the carbon source, it was observed that degree of cross-feeding from *B. xylanisolvens* on the growth of *B. ovatus* was structure-dependent. When fed on CAX, there was only minor increase in growth when *B. ovatus* was co-cultured with *B. xylanisolvens*, likely because *B. ovatus* utilizes CAX well and cross-feeding was not necessary (Fig. 4.4a). When the more structurally complex $CAXH_2$ was used as substrate, the difference between the growth of *B. ovatus* with and without *B. xylanisolvens* was considerable, showing that the supportive effect for *B. ovatus* growth increases when the necessity arises (Fig. 4.4b).

4.4.4 Structural features of corn arabinoxylan substrates

4.4.4.1 Molecular size distribution of corn arabinoxylan hydrolyzates

Molecular size distribution indicated a discrete structure of the $CAXH_2$ related to the combination of enzyme and bacteria hydrolysis. For the enzymatic treatment, $CAXH_2$ served as the core resistant structure resulting from hydrolysis of the simpler structures of CAX; while for *B. ovatus* treatment, $CAXH_2$ was further hydrolyzed into smaller fragments that the strain was unable to digest further(CAXH-digest), and which were found to provide no further nutrition to *B. ovatus* (Fig. 4.1b).

4.4.5 Structural patterns in arabinoxylan substrates that favor/disfavor *B. ovatus* growth

From neutral sugar compositional analysis, monomeric units of corn arabinoxylan hydrolysates were predominantly xylose and arabinose followed by galactose (Table 4.1). The low arabinose amount of $CAXH_2$ (17.5%) compared to CAX (27.4%) simply shows the arabinofuranohydrolase effects of selective remove of single arabinose branches. For the CAXH-digest, which is the residue after *B. ovatus* enzyme digestion, xylose is the major sugar changed (reduced from 52.9 to 44.3%), which reveals that the minor part of $CAXH_2$ that *B. ovatus* could hydrolyze was xylosyl residues.

Arabinoxylan contains a linear backbone chain of (1, 4)-*β*-D-xylopyranose residues with a base feature of single arabinofuranose units attached through 2-O and/or 3-O to xylose residues. In comparing CAX to $CAXH_2$, there was a marked decrease in terminal arabinosyl (15.3% to 6.4%) branches and a lesser decrease in terminal xylosyl (22.9% to 18.9%) branches, representing a reduction in number of these simple monosaccharide branches in the structure of $CAXH_2$ (Table 4.2). At the same time, there was a decrease in monosubstituted xylose (→4 (Xyl*p*)1 →3↑) (7.4%) from 26.1% to 18.7% which is consistent with the change of terminal arabinose (8.9%) (Table 4.3). Interestingly, unlike wheat arabinoxylan or corn arabinoxylan, in corn arabinoxylan hydrolyzates, large amounts of →2(Ara*f*)1 →, →3(Ara*f*)1 → and →5(Ara*f*)1 → were found, demonstrating the existence of a high proportion of long branch chains, other than mainly terminal sugar substituents directly attached on the backbone. As a result, in Table 4.3, while the unsubstituted xylose increased in $CAXH_2$ (17.4%), the structures were still more difficult to be hydrolyzed by enzymes than CAX (11.9%). Considering the similar trend between

the number of increased long branches (particularly →3 (Ara*f*) 1→ from 3.6 to 10.0%) and unsubstituted xylose (from 11.9 to 17.4%), one possibility is there are structural patterns that long side chains and unsubstituted xylose residues have which protect the structure from hydrolysis by enzymes by *B. xylanisolvens* and *B. ovatus*, but which *B. cell* readily used.

In comparing the $CAXH_2$ to CAXH-digest substrates, decrease in unsubstituted xylose residues (from 17.4% to 10.8%) (Table 4.3) again implies that *B. ovatus* prefers the unsubstituted xylose units for growth in CAXH-digest. Compared to the enzymatic treatment above that produced $CAXH_2$ from CAX and increased unsubstituted xylose residues, after *B. ovatus* treatment the unsubstituted residues were decreased substantially from 17.4 to 10.8% (Table 3) showing that the structural patterns involving long branches and neighbored unsubstituted xylose, were broken down by *B. ovatus*. In addition, disubstituted xylose increased from 10.2% in $CAXH_2$ to 15.2% in CAXH-digest, indicating that *B. ovatus* has poor or no capability to utilize disubstituted residues, presumably being the reason why *B. ovatus* could not grow on CAXH-digest. The further increase of long branches in CAXH-digest →2 (Ara*f*) 1 →, →3 (Ara*f*) 1 → and →5 (Ara*f*) 1 →, showed a long branch chain dominated structure. The multi-layer structure of corn arabinoxylan were proposed based on the function of isolated enzymes and degradation of specific bacteria discussed above (Fig. 4.3).

4.4.6 Growth of bacterial species in the artificial microbial community is determined by structure features of dietary fiber substrates

Changes in the three-member artificial community composition were investigated based on the different substrates described and defined above. Forty-eight hour mixed-culture experiments were conducted using CAX, $CAXH_2$, and CAXH-digest. After tracking the growth of each bacterium, the proportional compositions were determined. *B. cell* had the greatest cell number of all bacteria on different arabinoxylan substrates, which was consistent with its strong growth in pure culture and co-cultures of the substrates. It was notable, though, that compared to growth on CAX, the proportional percent of *B. cell* decreased after fed on $CAXH_2$ and CAXH-digest. The reason could be cooperative cross-feeding of *B. ovatus* on *B. xylanisolvens* as observed in Figs. 4.4 and 4.5 allowing *B. ovatus* to grow even on the complex arabinoxylan-based structures it could not utilize well directly. This cooperativeness apparently allowed the two bacteria to better compete with *B. cell* and likely indicates an unseen benefit that *B. ovatus* was giving to *B. xylanisolvens*. When fed $CAXH_2$, the proportion of *B. xylanisolvens* after 48 h incubation decreased to only 19.3% which was lower than when fed either CAX (29.8%) or CAXH-digest (28.4%). The cause of its low growth on $CAXH_2$ is likely found in the fact that *B. xylanisolvens*' lag time was longer compared to the lag time on CAX, as reported in Chapter 3. To note, when on $CAXH_2$ and CAX the difference of lag phases between *B. xylanisolvens* and other two bacteria was much smaller than when on $CAXH_2$. The delayed growth of *B. xylanisolvens* explains its disadvantage on $CAXH_2$. For *B. ovatus*, it was reasonable that the proportional percentage increased on $CAXH_2$ and CAXH-digest compared to CAX (9.9%), considering

the supportive cross-feeding effect it gained from *B. xylan* as discussed above. *B. ovatus* performed best on $CAXH_2$, but not the CAXH-digest, likely because the structures released from *B. xylanisolvens* still had complex branch structures that *B. ovatus* is not well equipped to utilize. Given the better growth of *B. ovatus* on $CAXH_2$ than CAXH-digest and considerable supportive effect it received compared to CAX, the highest proportional percent of *B. ovatus* on $CAXH_2$ is reasonable. The results demonstrate that the growth of individual bacteria in human colon could be manipulated by understanding the behavior of target bacteria in a competitive environment and pure cultured growth profiles on selected dietary fiber structures. Finally, the proper dietary fiber structures for controlled performance of target bacteria are possible to be obtained for desired microbiota compositions.

4.4.7 Strategies of gut bacteria for survival and growth

As described above, we observed that different strategies were applied by individual bacterial member in the community based on the availability of given dietary fiber structures. On the most complex polymer, CAXH-digest, which *B. ovatus* could not grow on alone, it served as a cooperator of *B. xylanisolvens* for cross-feeding to survive it this harsh situation where *B. ovatus* does not have carbon source available in the environment. At the same time, *B. xylanisolvens* should get some benefits from such cooperation, such as the possibility that *B. ovatus* puts pressure on *B. cell* which allows *B. xylanisolvens* to thrive. This could be due to some unknown factor or factors that occur from the growth of *B. ovatus*, which benefit *B. xylanisolvens*' growth. *B. ovatus* is a strong

competitor of *B. cell* on simple arabinoxylan structures, because *B. ovatus* can utilize the substrate better (Xu, 2012). Since *B. cell* and *B. xylanisolvens* have good ability to digest simple arabinoxylan structures, competition between them would give the system balance.

B. cell shows strong utilization capability on both simple and complex arabinoxylan structures (Xu, 2012), though a change in its competitive role came from introduction of other bacteria into the environment. On complex structures ($CAXH_2$ and CAXH-digest), although *B. ovatus* and *B. xylanisolvens* survive via cooperation, *B. cell* is basically a dominator in the system, and in the artificial community studied it had provided no cooperation with *B. ovatus* in terms of cross-feeding.

The growth of *B. xylanisolvens* was sensitive to the change in fiber chemical structure and the other bacteria in the artificial community. On specific structures, the competitiveness of *B. xylanisolvens* was influenced to make it a strong or weak competitor (Chapter 3). On complex fiber structures, *B. xylanisolvens* helped the growth of *B. ovatus* and apparently received some benefit from that action.

4.5 Conclusions

Through use of a model artificial gut bacteria community to show competition to defined complex carbohydrate substrates, this study demonstrated that specific structural features that are critical for the growth of target gut bacteria, and moreover for microbiota compositions. Structural patterns involving single substituted xylose residues and may be unsubstituted neighbors were used to prevent the hydrolysis of isolated enzymes, but could be broken down by *B. ovatus*, a common member of human gut bacteria. Long branch

residues containing →2 (Ara*f*) 1 →, →3 (Ara*f*) 1 → and →5 (Ara*f*) 1 → that are disubstituted on the xylose backbone, were shown previously to be associated with the poor utilization by gut bacteria, especially *B. ovatus*. In order to survive on the complex fiber structures, *B. ovatus* cooperated with *B. xylanisolvens*, another xylan-degrading member, and benefited through cross-feeding. Dietary fibers with different structural features influenced the results of supportive or cooperative growth based on the complexity of glycemic linkage patterns. Moreover, in the artificial community, the role of each bacterial member was affected by given fiber structures. For instance, *B. ovatus* when fed comparatively simple structures it has strong ability to compete for substrate and does not enter into a cooperative cross-feeding arrangement. However, on a complex substrate designed to be fully un-utilizable by *B. ovatus*, cooperation with *B. xylanisolvens* was activated allowing it to survive. In the end, the final microbiota compositions were changed by the defined corn arabinoxylan substrates based on structure/function relationships discussed above. The results imply a mechanism to manipulate the microbiota by selecting dietary fiber with proper structural features.

4.6 References

AACC (2000). "Total dietary fiber - determined as neutral sugar residues, uronic acid residues, and Klason lignin (Uppsala method)." AACC International: Approved Methods of American Association of Cereal Chemists, 10th edition. St. Paul, MN: AACC International Press.

Benomar, S., et al. (2015). "Nutritional stress induces exchange of cell material and energetic coupling between bacterial species." Nature Comm **6**.

Canny, G. O. and B. A. McCormick (2008). "Bacteria in the intestine, helpful residents or enemies from within?" Infect Immun **76**(8): 3360-3373

Carpita, N. C., et al. (1989). "Linkage structure of fructans and fructan oligomers from Triticum-aestivum and Festuca-arundinacea leaves." J Plant Physiol **134**(2): 162-168.

Chassard, C., et al. (2008). "*Bacteroides xylanisolvens* sp nov., a xylan-degrading bacterium isolated from human faeces." Int J Syst Evol Microbiol **58**: 1008-1013.

De Vadder, F., et al. (2014). "Microbiota-generated metabolites promote metabolic benefits via gut-brain neural circuits." Cell **156**(1-2): 84-96.

Germerodt, S., et al. (2016). "pervasive selection for cooperative cross-feeding in bacterial communities." PLoS Comp Biol **12**(6).

Hamaker, B. R. and Y. E. Tuncil (2014). "A perspective on the complexity of dietary fiber structures and their potential effect on the gut microbiota." J Mol Biol **426**(23): 3838-3850.

Ley, R. E., et al. (2005). "Obesity alters gut microbial ecology." Proc Natl Acad Sci USA **102**(31): 11070-11075.

Ley, R. E., et al. (2006). "Microbial ecology - human gut microbes associated with obesity." Nature **444**(7122): 1022-1023.

Macfarlane, G. T., et al. (2008). "Bacterial metabolism and health-related effects of galacto-oligosaccharides and other prebiotics." J Appl Microbiol **104**(2): 305-344.

Macpherson, A. J. and N. L. Harris (2004). "Interactions between commensal intestinal bacteria and the immune system." Nature Rev Immunol **4**(6): 478-485.

Martens, E. C., et al. (2009). "Complex glycan catabolism by the human gut microbiota: the Bacteroidetes Sus-like paradigm." J Biol Chem **284**(37): 24673-24677.

McNulty, N. P., et al. (2013). "Effects of diet on resource utilization by a model human gut microbiota containing bacteroides cellulosilyticus WH2, a symbiont with an extensive glycobiome." PLoS Biol **11**(8).

Michlmayr, H., et al. (2013). "arabinoxylan oligosaccharide hydrolysis by family 43 and 51 glycosidases from lactobacillus brevis DSM 20054." Appl Environ Microbiol **79**(21): 6747-6754.

Mirande, C., et al. (2010). "Characterization of Xyn10A, a highly active xylanase from the human gut bacterium Bacteroides xylanisolvens XB1A." Appl Microbiol Biotechnol **87**(6): 2097-2105.

Qin, J. J., et al. (2010). "A human gut microbial gene catalogue established by metagenomic sequencing." Nature **464**(7285): 59-U70.

Rogowski, A., et al. (2015). "Glycan complexity dictates microbial resource allocation in the large intestine." Nat Commun **6**: 7481.

Sartor, R. B. (2008). "Microbial influences in inflammatory bowel diseases." Gastroenterology **134**(2): 577-594.

Seth, E. C. and M. E. Taga (2014). "Nutrient cross-feeding in the microbial world." Frontiers Microbiol **5**.

Whitehead, T. R. and R. B. Hespell (1990). "The genes for 3 xylan-degrading activities from *Bacteroides-ovatus* are clustered in a 3.8-kilobase region." J Bacteriol **172**(5): 2408-2412.

Xu, H. (2012). "Influence of the structural complexity of cereal arabinoxylans on human fecal fermentation and their degradation mechanism by gut bacteria." Ph.D. thesis, Purdue University.

4.7 Tables and Figures

Tables

Table 4.1 Composition of corn arabinoxylan hydrolyzates.[a]

Constituent	CAX	$CAXH_2$	CAXH-digest
Arabinose	27.4±1.9	17.5±0.7	15.0±1.4
Xylose	51.2±3.0	52.9±1.8	44.3±1.9
Galactose	7.5±0.2	10.8±0.8	9.9±0.5
A/X ratio	0.54	0.33	0.34

[a] Means ± standard error. See Table 2.1 for abbreviations.

Table 4.2 Glycosidic linkage composition [mol%] of corn arabinoxylan hydrolyzates. [a]

Component	Linkage indicated	CAX	$CAXH_2$	CAXH- digest
2,3,5-Me_3-Ara	(Ara*f*)1→	15.3±0.4	6.4±0.5	5.8±0.3
3,5-Me_2-Ara	→2(Ara*f*)1 →	3.5±0.5	5.5±0.2	6.5±0.2
2,5-Me_2-Ara	→3(Ara*f*)1 →	3.6±0.2	10.0±0.4	12.5±0.6
2,3-Me_2-Ara	→5(Ara*f*)1 →	1.4±0.6	3.9±0.1	5.0±0.3
2,3,4-Me_3-Xyl	(Xyl*p*)1→	22.9±2.1	18.9±0.6	20.3±1.9
2,3-Me_2-Xyl	→4(Xyl*p*)1 →	11.9±0.7	17.4±0.3	10.8±0.8
2-Me_1-Xyl	→4(Xyl*p*)1 →3↑	26.1±1.1	18.7±0.4	19.7±1.1
Xyl	→4(Xyl*p*)1 →3↑↑2	11.9±0.5	10.2±0.6	15.2±0.9
2,3,4,6-Me_4-Gal	(Gal*p*)1→	3.4±0.1	6.1±0.3	5.4±0.6

[a] Values are expressed as a proportion of all partially methylated alditol acetates present.

See Table 2.1 and 2.2 for abbreviations.

Table 4.3 Percent substitution of xylopyranosyl residues in the xylan backbone of arabinoxylan samples. [a]

Component	CAX	$CAXH_2$	CAXH-digest
Unsubstituted xylose	11.9±0.7	17.4±0.3	10.8±0.8
Monosubstituted xylose	26.1±1.1	18.7±0.4	19.7±1.1
Disubstituted xylose	11.9±0.5	10.2±0.6	15.2±0.9

[a] Means ± standard error. See Table 2.1 for abbreviations.

Figures

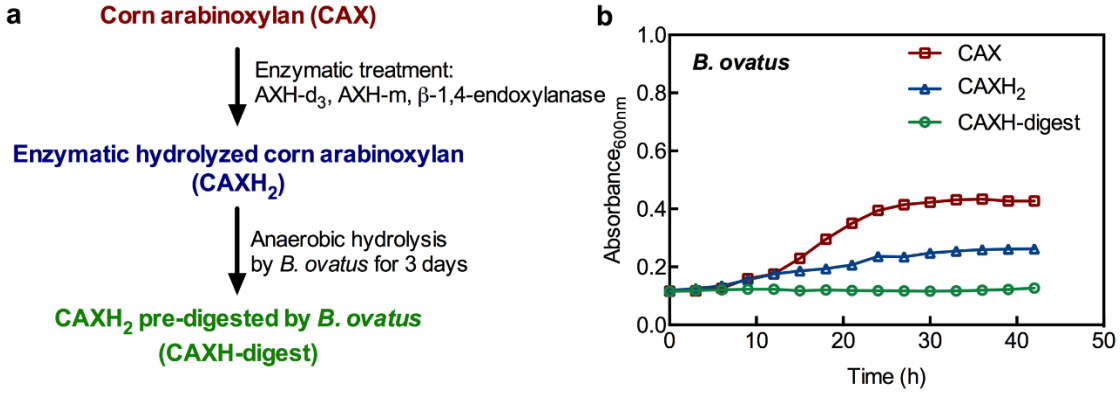

Figure 4.1 a) Preparation of arabinoxylan fragments from enzymatic treatments and bacterial hydrolysis. b) Growth curves of *Bacteroides ovatus* on CAX (red), $CAXH_2$ (blue) and CAXH-digest (green) at OD_{600} nm.

See Table 2.1 for abbreviations.

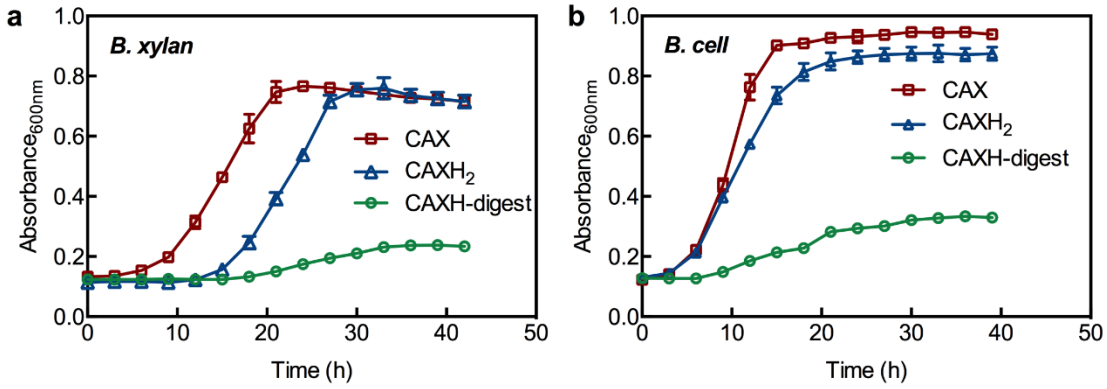

Figure 4.2 Growth curves of *B. xylan* a) and *B. cell* b) on different arabinoxylan substrates: CAX (red), $CAXH_2$ (blue), and CAXH-digest (green).

See Table 2.1 for abbreviations.

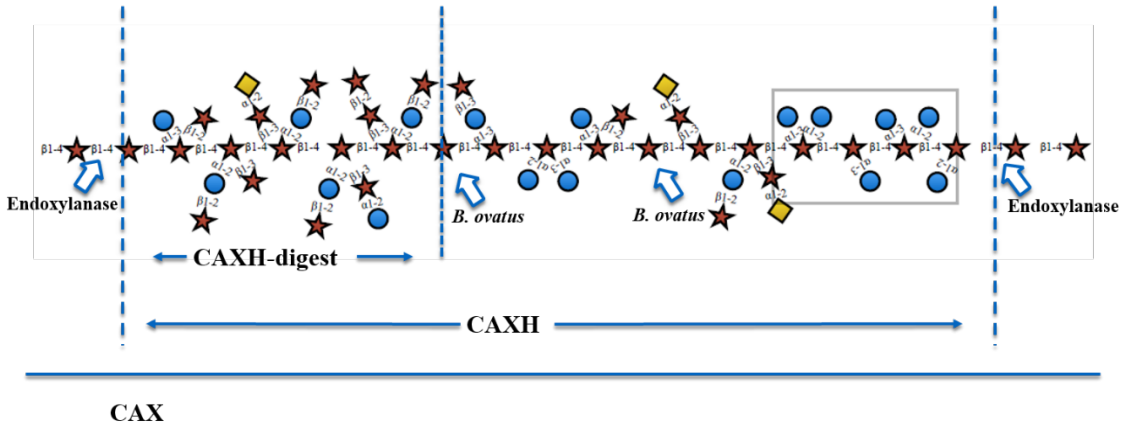

Figure 4.3 Structural layers in CAX for isolated enzyme treatment and bacterial (*B. ovatus*) treatment.

See Table 2.1 for abbreviations.

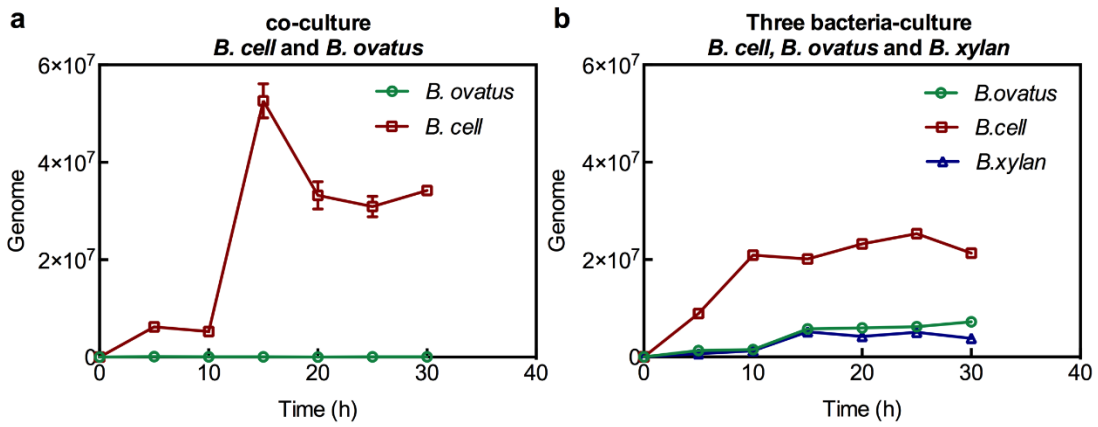

Figure 4.4 Growth curves of bacteria in mixed-cultures on CAXH-digest. a) *B. cell* (red) and *B. ovatus* (green) grown together on CAXH-digest. b) *B. cell* (red), *B. ovatus* (green) and *B. xylan* (blue) grown together on CAXH-digest.

See Table 2.1 for abbreviations.

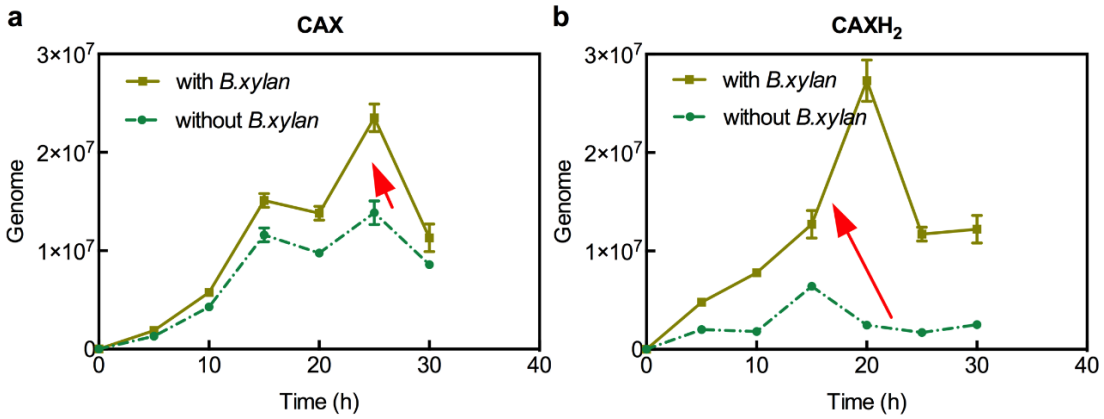

Figure 4.5 Growth change of *B. ovatus* on CAX a) and $CAXH_2$ b) with and without *B. xylan*.

See Table 2.1 for abbreviations.

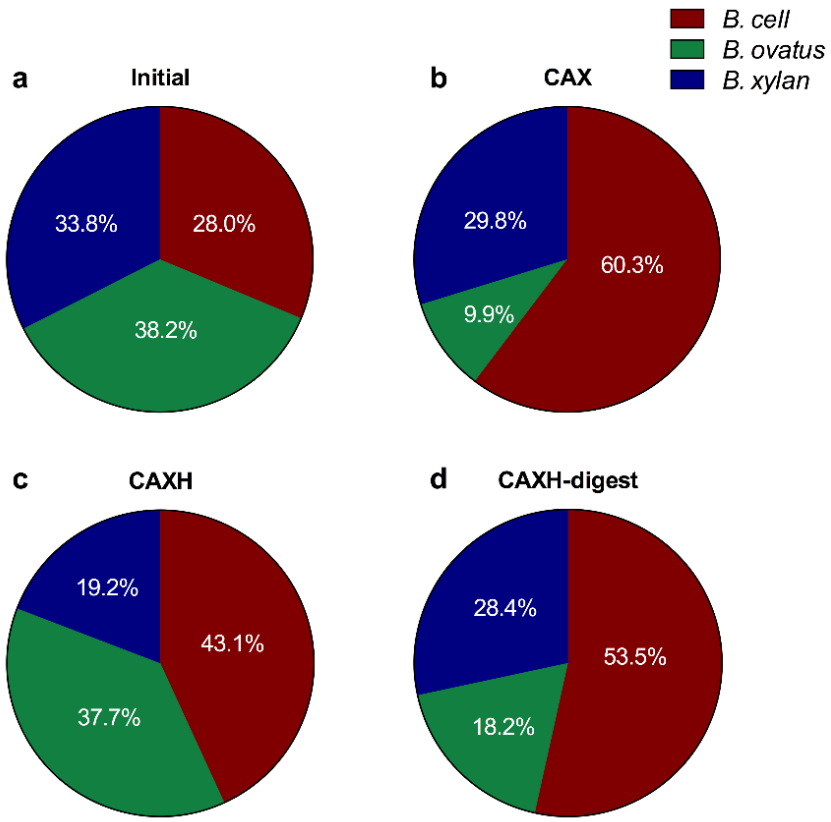

Figure 4.6 Microbiota compositions of a three bacteria artificial community after 48 h on CAX, $CAXH_2$, and CAXH-digest (red *B. cell*, blue *B. xylan*, green *B. ovatus*). a) Initial composition (0 h). b) Bacteria grown on CAX after 48 h. c) Bacteria grown on $CAXH_2$ after 48 h. d) Bacteria grown on CAXH-digest after 48 h. See Table 2.1 for abbreviations.

OVERALL CONCLUSIONS

This thesis explored the connections between dietary fiber structural features and change of gut bacterial growth in pure and multi-bacterial experiments. Arabinoxylan from corn bran was applied as the model fiber structure and gut bacteria from the genus *Bacteroides* as target bacteria. Compared to molecular size or arabinose/xylose ratio, a previous study had indicated that the branch patterns in dietary fiber play a significant role in bacterial fermentation. In the first part of the thesis research, a variety of corn arabinoxylan hydrolyzates were prepared with different structural features, particularly branch features, and used for the following studies. Branch type (mono- and disaccharide branches) and how the branches attach on the backbone were analyzed and described the complexity of dietary fiber branches, which are related to the difficulty of degradation and utilization by gut bacteria. Moreover, linkage patterns were investigated with the specific change of target bacterial growth, which may refer to recognition and binding of structures in the early phase of the digestion in gut bacteria.

In the second study, a highly specific relationship was drawn between CAX hydrolyzates and the growth of the gut bacteria. Subtle changes on arabinosyl substituents in corn arabinoxylan hydrolyzates such as $CAXH_1$ and $CAXH_2$ were found to induce a substantial lag time change of *B. xylanisolvens*. The structural difference came from the

different sequence of debranching and backbone enzymatic treatments. In $CAXH_2$, the linkage patterns involving more disubstituted arabinosyl branches increased indicating a more complex structure compared to $CAXH_1$. The study shows that the lag phase shift of *B. xylanisolvens* can be modulated by subtle changes in structural patterns of arabinoxylan, specifically the arabinosyl side chain type and distribution in CAX hydrolysate structures. A multi-bacterial experiment indicated that the competitiveness of *B. xylanisolvens* was, in turn, decreased due to longer lag time on $CAXH_2$. Expression of CAX-hydrolysate utilization related genes in *B. xylanisolvens* mirrored the growth response to changes in structural features of the corn AX molecules. Further study revealed that density of the molecular structure of arabinoxylan molecules is another important feature for the lag phase change. Loose structures reduced the effect of lag phase shift. In the future, this finding may contribute to design proper fiber ingredients for promotion or suppression of target gut bacteria through change in competitiveness.

In the third study, the interactions between gut bacteria were investigated which are of significance for microbiota community structures on given dietary fiber structures. In order to survive on a complex fiber structure that it cannot utilize alone, *B. ovatus* cooperated with *B. xylan*, another xylan-degrading member, and benefited through cross-feeding. Dietary fibers with different structural features influenced the results of supportive or cooperative (cross-feeding) growth based on the complexity of glycemic linkage patterns. Moreover, in the artificial community, the role of each bacterial member was affected by given fiber structures. For instance, *B. ovatus*, when fed comparatively simple structures, has strong ability to compete for substrate and did not enter into a cooperative cross-feeding arrangement. However, on a complex substrate, designed to be fully un-

utilizable by *B. ovatus*, cooperation with *B. xylanisolvens* was activated allowing it to survive. Therefore, the performance of microbial members in the community was influenced by fiber structure-dependent changes. Further study on microbial community structure with large bacterial numbers will be required. In the end, this work implies a direction of positive manipulation of gut microbiota composition based on structure/function relationships of dietary fiber.

VITA

VITA

Xin Nie received his Bachelor of Science degree in Chemistry from China Agricultural University, Beijing, P. R. China in July, 2008. Then he studied as a Master student in the chemistry department of China Agricultural University till July, 2011. In August 2011, Xin Nie was enrolled as a Ph.D. student in Food Science Department, Purdue University. Under the guidance of Dr. Bruce R. Hamaker, his research focused on investigation of the structure/function relationship of dietary fiber on the influence of human health through manipulation of gut microbiota.